Faculty of Science and Applied Science
Department of Mechanical Engineering

FINAL PROJECT

Presented for the attainment of the Master's Degree
Specialization: Mechanical Engineering
Option: Energetic

THEME

Computational analysis of the natural convection phenomena occurring in partially heated square enclosures filled with nanofluids

By :

ACHIT MEROUANE

YANINA YASSER EL MOTASSEM

Thesis examination committee:

Pr. Mahfoud Brahim	Superviser
Pr. Laouari Azzedine	President
Pr. Bensalem Chafik	Examiner

2023/2024

الجمهورية الجزائرية الديمقراطية الشعبية
République Algérienne Démocratique et Populaire

Ministère de l'Enseignement Supérieur
et de la Recherche Scientifique
Université Akli Mohand Oulhadj - Bouira -
ⵜⴰⵙⴷⴰⵡⵉⵜ ⴰⴽⵍⵉ ⵎⵓⵃⴻⵏⴷ ⵓⵍⵃⴰⵊ - ⵜⵓⴱⵉⵔⴻⵜ -
Faculté des Sciences et des Sciences Appliquées

وزارة التعليم العالي والبحث العلمي
جامعة أكلي محند أولحاج
- البويرة -
كلية العلوم والعلوم التطبيقية

جامعة البويرة

Génie mécanique

Spécialité : Energétique

Autorisation de déposer un mémoire de Master pour soutenance

Je soussigné, l'enseignant (e) : .....Pr.Mahfoud Brahim

L'encadreur du mémoire de fin d'études des étudiants :

1.ACHIT MEROUANE

2.YANINA YASSER EL MOTASSEM

Ayant le mémoire de fin d'études de Master intitulé : Computational analysis of the natural convection phenomena occurring in partially heated squar enclosures filled with nanofluids

Promotion : 2023/ 2024

Et après voir et consulté le mémoire dans sa forme finale j'autorise les étudiants à l'imprimer et la déposer pour la soutenance.

Bouira le : 13/06/2024

Signature du L'encadreur

Signature du chef de département

مساعد رئيس قسم الهندسة الميكانيكية
مكلف بالتدريس والتأطير في الدكتوراه
أ. مسعود فارق

الجمهورية الجزائرية الديمقراطية الشعبية
Republique Algerienne Democratique et Populaire

وزارة التعليم العالي و البحث العلمي
جامعة أكلي محند أولحاج - البويرة

Ministère de l'Enseignement Supérieur
et de la Recherche Scientifique
Université Akli Mohand Oulhadj - Bouira
Tasdawit Akli Muhend Ulhağ - Tubirett

نموذج التصريح الشرفي الخاص بالالتزام بقواعد النزاهة العلمية لإنجاز بحث.

انا الممضي اسفله،

السيد(ة) ..... الصفة: طالب، استاذ، باحث .....

الحامل(ة) لبطاقة التعريف الوطنية: ..... والصادرة بتاريخ .....

المسجل(ة) بكلية / معهد ..... قسم .....

والمكلف(ة) بإنجاز اعمال بحث(مذكرة، التخرج، مذكرة ماستر، مذكرة ماجستير، اطروحة دكتوراه).

عنوانها: .....

تحت إشراف الأستاذ(ة): .....

أصرح بشرفي اني ألتزم بمراعاة المعايير العلمية والمنهجية الاخلاقيات المهنية والنزاهة الاكاديمية المطلوبة في انجاز البحث المذكور أعلاه.

التاريخ: .....

توقيع المعني(ة)

رأي هيئة مراقبة السرقة العلمية:

النسبة: % .....

الامضاء:

الجمهورية الجزائرية الديمقراطية الشعبية
République Algérienne Démocratique et Populaire

وزارة التعليم العالي و البحث العلمي
جامعة أكلي محند أولحاج - البويرة

Ministère de l'Enseignement Supérieur
et de la Recherche Scientifique
Université Akli Mohand Oulhadj - Bouira
Tasdawit Akli Muhend Ulhağ - Tubirett

نموذج التصريح الشرفي الخاص بالالتزام بقواعد النزاهة العلمية لإنجاز بحث.

انا الممضي اسفله،

السيد(ة) بوسنة ياسر الحسين الصفة: طالب، استاذ، باحث طالب

الحامل(ة) لبطاقة التعريف الوطنية: 404217536 والصادرة بتاريخ 2023/06/03

المسجل(ة) بكلية / معهد العلوم والعلوم التطبيقية قسم هندسة ميكانيكية

والمكلف(ة) بإنجاز اعمال بحث(مذكرة، التخرج، مذكرة ماستر، مذكرة ماجستير، اطروحة دكتوراه).

عنوانها: computational analysis of the natural convection phenomena occurring in partially heated square enclosure filled with nanofluids

تحت إشراف الأستاذ(ة): محفوظ براهيم

أصرح بشرفي اني ألتزم بمراعاة المعايير العلمية والمنهجية الاخلاقيات المهنية والنزاهة الاكاديمية المطلوبة في انجاز البحث المذكور أعلاه.

التاريخ: 17/07/2024

توقيع المعني(ة)

رأي هيئة مراقبة السرقة العلمية:

النسبة: % 25

الامضاء:

جامعة أكلي محند اولحاج - البويرة
قسم
ميكانيك

ACKNOWLEDGEMENTS

We express our gratitude to Allah (SWT) for the courage and will that made this study possible.

We also wish to extend our sincere thanks to our beloved parents for their support and guidance throughout these years of study.

First and foremost, we would like to express our deep appreciation to our supervisor, Dr. Mahfoud Brahim, for his invaluable assistance, availability, kindness, and valuable guidance throughout this work. Without his methodology, guidance, and wise counsel, this study would not have been possible.

We wish to express our sincere thanks to the members of the jury for their interest in our research by agreeing to evaluate our work and enrich it with their suggestions.

Finally, we would like to express our gratitude to all those who have contributed directly or indirectly to the completion of this work. Their support and participation have been invaluable.

DEDICATION

I DEDICATE THIS THESIS:

TO MY DEAR PARENTS, MY FATHER AND MY MOTHER, FOR THEIR PATIENCE, THEIR LOVE, THEIR SUPPORT, AND THEIR ENCOURAGEMENT.

TO MY BROTHER ADEM AND SISTER.

TO MY ENTIRE FAMILY.

TO ALL MY FRIENDS.

NOT FORGETTING TO MENTION ALL THE TEACHERS AND ALL THE EMPLOYEES IN THE MECHANICAL ENGINEERING DEPARTMENTS.

YANINA YASSER EL MOTASSEM

DEDICATION

I DEDICATE THIS THESIS

TO MY DEAR PARENTS, MY MOTHER AND MY FATHER, FOR THEIR PATIENCE, LOVE, SUPPORT, AND ENCOURAGEMENT. TO MY BROTHERS AND MY SISTER, AND TO MY ENTIRE FAMILY. I ALSO WANT TO EXPRESS MY GRATITUDE TO ALL MY FRIENDS. LET'S NOT FORGET TO MENTION ALL THE TEACHERS FROM THE MECHANICAL ENGINEERING DEPARTMENT, WHOSE WORK AND CONTRIBUTION HAVE BEEN INVALUABLE. THANK YOU ALL FOR YOUR INVALUABLE SUPPORT.

ACHIT MEROUANE

ملخص

تمت دراسة تأثير الحمل الحراري الطبيعي في حاويات مربعة مسخنة ومملوءة بالسوائل النانوية، بهدف فهم تأثير الجسيمات النانوية والحقل المغناطيسي على انتقال الحرارة داخل هذه الحاويات. تم اختيار السوائل النانوية، مثل أكسيد الألمنيوم والنحاس، بنسبة حجم صلبة محددة .(ϕ=0.03) وقد قمنا بتحليل تأثير قيم عدد رايلي ($Ra=10^4,10^5,10^6$) وعدد هارتمان (Ha=0, 30, 60) على توزيعات التدفق ودرجات الحرارة داخل الحاوية. أظهرت النتائج أن زيادة قيم عدد رايلي تؤدي إلى زيادة في قيم عدد هارتمان، ويعزى ذلك إلى زيادة التدفق والاختلاط داخل الحاوية نتيجة لتحركات السائل النانوي المحسنة، مما يسهم في زيادة انتقال الحرارة داخل الحاوية.

Résumé

L'effet de la convection naturelle dans des contenants carrés chauffés remplis de nanofluides a été étudié afin de comprendre l'impact des nanoparticules et des champs magnétiques sur le transfert de chaleur à l'intérieur de ces contenants. Des nanofluides tels que l'oxyde d'aluminium et le cuivre, avec une fraction volumique solide fixe (ϕ=0,03), ont été choisis. Nous avons analysé les effets des valeurs du nombre de Rayleigh ($Ra=10^4$, 10^5, 10^6) et des valeurs du nombre de Hartmann (Ha=0, 30, 60) sur les distributions de flux et les gradients de température à l'intérieur du contenant. Les résultats ont indiqué qu'une augmentation du nombre de Rayleigh entraînait une augmentation des valeurs du nombre de Hartmann, attribuée à un mouvement et à un mélange améliorés des fluides à l'intérieur du contenant en raison d'une meilleure circulation des nanofluides, contribuant ainsi à un transfert de chaleur accru à l'intérieur du contenant.

Abstract

The effect of natural convection in square heated containers filled with nanofluids has been studied to understand the impact of nanoparticles and magnetic fields on heat transfer within these containers. Nanofluids such as aluminum oxide and copper, with a fixed solid volume fraction (ϕ=0.03), were chosen. We analyzed the effects of Rayleigh number values ($Ra=10^4$, 10^5, 10^6) and Hartmann number values (Ha=0, 30, 60) on flow distributions and temperature gradients inside the container. The results indicated that an increase in Rayleigh number led to an increase in Hartmann number values, attributed to enhanced fluid movement and mixing within the container due to improved nanofluid circulation, thereby contributing to increased heat transfer within the container.

Summary

List of figures

List of Tables

Nomenclature

b :length of the heat source [m].

B : dimensionless length of the heat source (b/l).

d :the distance between the heat source and the left wall [m].

D : la distance adimensionnelle entre la source de chaleur et ma paroi gauche(d/L).

T_C: temperature [K].

T_S :temperature of the source [K].

T_∞: ambient temperature [K] .

L : length of the cavity [m].

Pr :Prandtl number $Pr = \frac{\upsilon}{\alpha}$.

Nu :"Nusselt number . $Nu = \frac{hl}{k_f}$.

Ra :Rayleigh number .$Ra = \frac{g\beta L^3(Th-Tc)}{\upsilon\alpha}$.

Ha :Hartmann number $Ha = B_0 L\sqrt{\frac{\sigma}{\rho\upsilon^-}}$.

B :length of the heat source [m].

g :acceleration due to gravity[m.s^2].

h : convective heat transfer coefficient

p: pressure [Nm-2].

p: modified pressure [Nm-2]. t: time [s].

CP: specific heat at constant pressure [J.kg-1.K-1].

V: volume [m3].

m: mass [kg].

q″: heat flux from the source per unit area [W/m²].

SΦ: source term.

K: thermal conductivity [W.m-1.K-1].

u, v: velocity components in the x, y directions [m/s].

U, V: dimensionless velocity components (uL/af, vL/af).

x, y: Cartesiancoordinates [m].

X, Y: dimensionlesscoordinates (x/L; y/L).

Δx: change in x [m].

Δy: change in y [m].

Greek symbols:

a: thermal diffusivity [m²/s].

β: coefficient of thermal expansion at constant pressure [K-1].

μ: dynamic viscosity [kg.m-1.s-1].

ν: kinematic viscosity [m²/s].

ρ: density [kg.m-3]

ψ: dimensionless stream function.

ΔT: temperature difference.

θ: dimensionless temperature.

Ω: dimensionlessvorticity.

σ:sigma

Ø: volume fraction.

Φ: dependent variable.

The clues :

nf: nano-fluid.

p: particle.

f: base fluid.

c: hot.

Max: maximum.

Red: nano-fluid.

Green: water.

Orange: hot.

Blue: cold.

i: in the x direction.

j: in the y direction.

n: iteration index.

*: estimated value.

': Correction index or fluctuations.

General Introduction

General Introduction

When the fluid is electrically conductive and exposed to a magnetic field, the Lorentz force is also activated and interacts with the buoyancy force so that the flux and temperature fields are governed. The use of an external magnetic field is increasingly employed in the nanotechnology industry as a control mechanism, as convection currents are suppressed by the Lorentz force, thereby reducing velocities. The study and thorough understanding of the transfer of momentum and heat in such a process are crucial for improving control and the quality of manufactured products.

Indeed, the objectives of this work are to study magnetohydrodynamic convection in a square enclosure containing a nanofluid (Al_2O_3-water) and (Cu- water) and subjected to a magnetic field. Mathematical models governing these phenomena have been developed. Additionally, numerical simulations have been performed. The simulations were conducted using the Fluent software (student version).

This thesis is structured as follows:

• The first chapter is dedicated to presenting a literature review as well as the theory of the main published works in the field of heat transfer in cavities.

• The second chapter is dedicated to proposing the mathematical model, initial conditions, and boundaries, in a two-dimensional situation (x-y).

• The third chapter focuses on describing the finite volume method, as well as the numerical discretization of the general transport equation, and a presentation of the calculation code - FLUENT.

• Chapter four gathers the validation of our calculation program as well as the main numerical results of this study. Comments, interpretations, and analyses of the various results of this parametric study are also presented.

• Finally, a general conclusion summarizing the main results obtained is given at the end of this thesis.

Chapter I : Introduction and Bibliographic Research

Chapter I : Introduction and Bibliographic Research

I.1.Introduction

In the first chapter, we embark on an exhaustive exploration and retrospective analysis of natural convection phenomena within partially heated square enclosures filled with nanofluids. This introductory discourse is aimed at elucidating crucial definitions while providing a broader perspective on nanofluids as an intriguing subset of fluids.

Within this preliminary investigation, we delve into the historical lineage of natural convection in such enclosures, spotlighting the trajectory of advancements and seminal discoveries that have shaped our contemporary understanding of this intricate phenomenon. Following this historical backdrop, we proceed to offer precise and comprehensive definitions pertaining to the key concepts and terminologies that form the foundation of our study. Additionally, we undertake a detailed examination of the intrinsic characteristics of nanofluids, shedding light on their properties and significance within the context of our research framework.

I.2.Review bibliographies:

Convective heat transfer can be enhanced passively by changing flow geometry, boundary conditions, or by enhancing thermal conductivity of the fluid. Various techniques have been proposed to enhance the heat transfer performance of fluids. Researchers have also tried to increase the thermal conductivity of base fluids by suspending micro- or larger-sized solid particles in fluids since the thermal conductivity of solid is typically higher than that of liquids. Numerous theoretical and experimental studies of suspensions containing solid particles have been conducted since Maxwell's theoretical work was published more than 100 years ago [1]. However, due to the large size and high density of the particles, there is no good way to prevent the solid particles from settling out of suspension. The lack of stability of such suspensions induces additional flow resistance and possible erosion. Hence, fluids with dispersed coarse-grained particles have not yet been commercialized. Modern nanotechnology provides new opportunities to process and produce materials with average crystallite sizes below 50 nm. Fluids with nanoparticles suspended in them are called nanofluids, a term proposed by Choi in 1995 of the Argonne National Laboratory, U.S.A. [2]. Nanofluids can be considered the next-generation heat transfer fluids as they offer exciting new possibilities to enhance heat transfer performance compared to pure liquids. They are expected to have

superior properties compared to conventional heat transfer fluids, as well as fluids containing micro-sized metallic particles. The much larger relative surface area of nanoparticles, compared to those of conventional particles, should not only significantly improve heat transfer capabilities, but also should increase the stability of the suspensions. Also, nanofluids can improve abrasion-related properties as compared to the conventional solid/fluid mixtures. Successful employment of nanofluids will support the current trend toward component miniaturization by enabling the design of smaller and lighter heat exchanger systems. Keblinski et al. [3] made an interesting simple review to discuss the properties of nanofluids and future challenges. The development of nanofluids is still hindered by several factors such as the lack of agreement between results, poor characterization of suspensions, and the lack of theoretical understanding of the mechanisms. Suspended nanoparticles in various base fluids can alter the fluid flow and heat transfer characteristics of the base fluids. Necessary studies need to be carried out before wide application can be found for nanofluids. In this paper we present an overview of the literature dealing with recent developments in the study of heat transfer using nanofluids. First, the preparation of nanofluids is discussed; this is followed with a review of recent experimental and analytical investigations with nanofluids.

I.3Definition:

I.3.1 Definition of nanofluids:

Nanofluids represent colloidal suspensions comprising dispersed nanoparticles within a matrix of a fundamental fluid. These nanoparticles, typically within the range of a few to tens of nanometers, are commonly denoted as ultrafine particles (UFP). Nanostructured particles are elemental constituents with dimensions confined between 1 and 100 nanometers (one nm = 10^-9 m = 0.000000001 m) and are fabricated from materials such as metals, oxides, or carbonates. Nanofluids exhibit superior thermophysical characteristics compared to their base counterparts, including heightened thermal conductivity and augmented heat transfer coefficients. These distinctive attributes render nanofluids auspicious candidates for diverse applications, encompassing electronic system cooling and industrial heat exchange optimization. The fine-tuning of nanofluid properties via compositional adjustments, concentration modulation, and nanoparticle size manipulation heralds novel prospects for thermal engineering and the development of cutting-edge, high-performance devices.

- **The nanoparticles:**

Also referred to as ultrafine particles (PUF), nanoparticles are molecules with sizes ranging from one to one hundred nanometers (1 nm = 10-9 m = 0.000000001m).They are therefore smaller than a cell and larger than atoms.

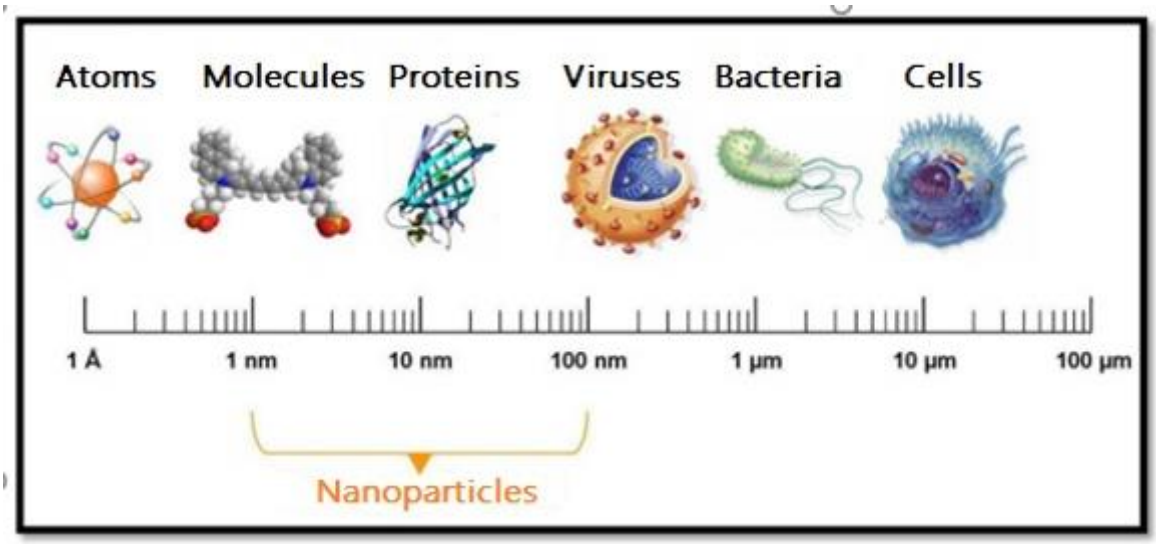

Figure I. 1. Nano molecule scale

Nanoparticles have many preparation processes that can be classified into two categories :

- physical processes, such as mechanical grinding.
- chemical processes, such as pyrolysis or chemical precipitation.

The most used nanoparticles to obtain nano fluids are :

- **The nanoparticles of metal oxides**

  Aluminum oxide (Al2O3)

  Copper oxide (CuO)

  Silicon oxide (SiO2)

  Titanium oxide (TiO2)

- **The metal nanoparticles**

  Aluminum (Al)

  Copper (Cu)

  Gold (Ag)

- **The non-metallic nanoparticles**

The carbon nanotube (CNT), The diamante (C)

Refrigerating fluids (R12, R22)

Table I. 1. The thermophysical properties of the different materials

	Nanoparticle and fluid basic	K (W /m K)	ρ (Kg/m3)	Cp (J/ Kg K)	μ (Pa. s)
Metallic (solid)	Cu	400	8954	383	
	Fe	80,2	7870	447	
	Ni	90,7	8900	444	
	Au	317	19,300	129	
	Ag	429	10,500	235	
	C (diamond)	2300	3500	509	
Oxide Metallic (solid)	SiO2	1,38	2220	745	
	TiO2	8,4	4157	710	
	Al2O3	36	3970	765	
	CuO	69	6350	535	
	SiC	490	3160	675	
Liquids No metallic	The water	0,613	1000	4183	0,0008
	Ethylene glycol (EG)	0,258	1132	2349	513
					0,0157

I.3.2 Natural convection:

Natural convection refers to a fundamental aspect of fluid dynamics wherein fluid motion arises due to temperature differences, causing vertical movement within the fluid. This phenomenon occurs spontaneously as a result of the buoyancy force, commonly known as the Archimedes principle. When a fluid undergoes thermal changes, its density alters, becoming either lighter or denser compared to the surrounding fluid. This density disparity initiates convective motions, wherein the fluid moves vertically, redistributing heat and altering the fluid's characteristics. Natural convection phenomena are prevalent in various natural processes, including the formation of ocean currents, the development of thunderstorms in

meteorology, and the movement of magma in geology, illustrating its widespread importance across different scientific disciplines.

I.3.3 Thermal conductivity:

The thermal conductivity is a property that measures how well a material conducts heat. It shows how heat moves through a material when the ends are, at temperatures. Thermal conductivity is typically measured in watts per meter kelvin (W/(m·K)). Tells us how fast heat travels through a substance.

Different fluids have varying conductivities. For instance;

1. Water; 0.606W/(m·K)

2. Air; Around 0.0257W/(m·K)

3. Engine Oil; 0.135 W/(m·K)

4. Solid Aluminum; 237 W/(m·K)

5. Solid Copper; 398 W/(m·K)

6. Argon Gas; 0.0163W/(m·K)

7. Solid Glass; Around 1 W/(m·K)

8. Silicone Polymer; 0.15W/(m·K)

These values are estimates. Can vary based on factors, like temperature and the specific composition of the fluid.

I.4 Electrical conductivity

Electrical conductivity, also known as electrical conductance, measures the ability of a material to allow the passage of electric current. It indicates how easily electric charges (usually electrons) move through a material when an electrical potential difference is applied between its ends. Electrical conductivity is expressed in siemens per meter (S/m) and is inversely proportional to the electrical resistance of a material. Conductive materials such as metals have high electrical conductivity, while insulators have low electrical conductivity.

I.5 Preparation of nano-fluid:

The process of creating nanofluids involves more than just blending the nanoparticles with the basic fluid. Stabilization and appropriate mixing are necessary in specific environmental conditions to produce nanofluids with uniformly distributed nanoparticles.

Nanofluids can be prepared using a variety of techniques, notably can be divided further into two main categories:

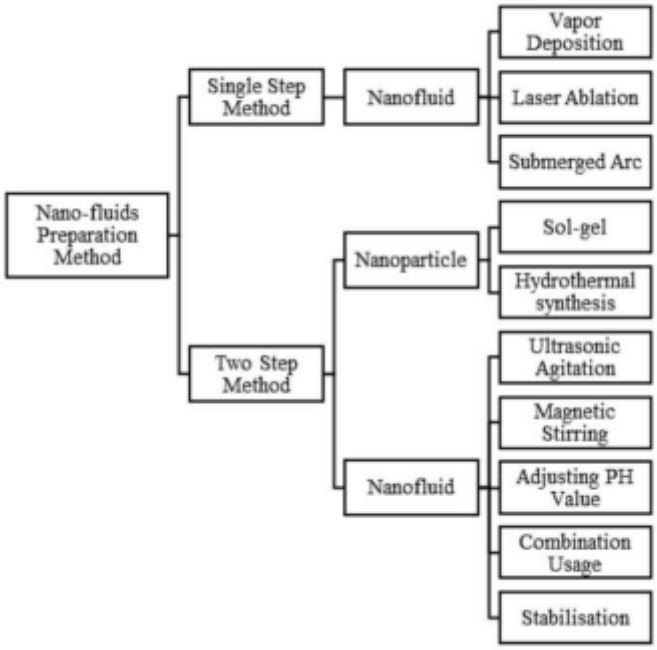

Figure I. 2 . Techniques for creating nanofluids

- **One-step method:**

It involves the vaporization of a solid material under vacuum and its direct condensation in the liquid. The solid material is transformed into steam, condensed in the liquid and dispersed in the form of nanoparticles. This approach has the advantage of producing nanofluids directly, but it can also be complex to control in terms of particle size and distribution.

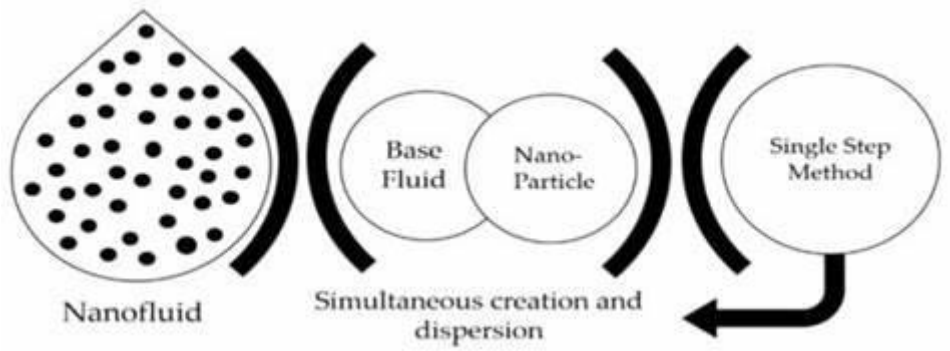

Figure I. 2. One-Step Method

- **Two-step method:**

This method first begins by creating a powder of Nano dimensioned solids, which are then mixed and dispersed into a base fluid. With this approach, nanoparticles are first made in the solid form and then added into the liquid. This makes it slightly less messy and gives a better control of particle sizes, but it is two-step.

Manufacturing processes can be of a physical nature or a Chemical. They are the subject of continuous research to optimize the cost of production, which can sometimes be high due amount of energy and high temperatures required and due insurmountable challenges associated with the implementation and obtaining the desired size of the particles, and the resultant batch inhomogeneity. To know whether each method of the disadvantages and some may not be suitable for the scale of mass nanoparticle production, due to the constraints related to the specific process, especially for one-step methods.

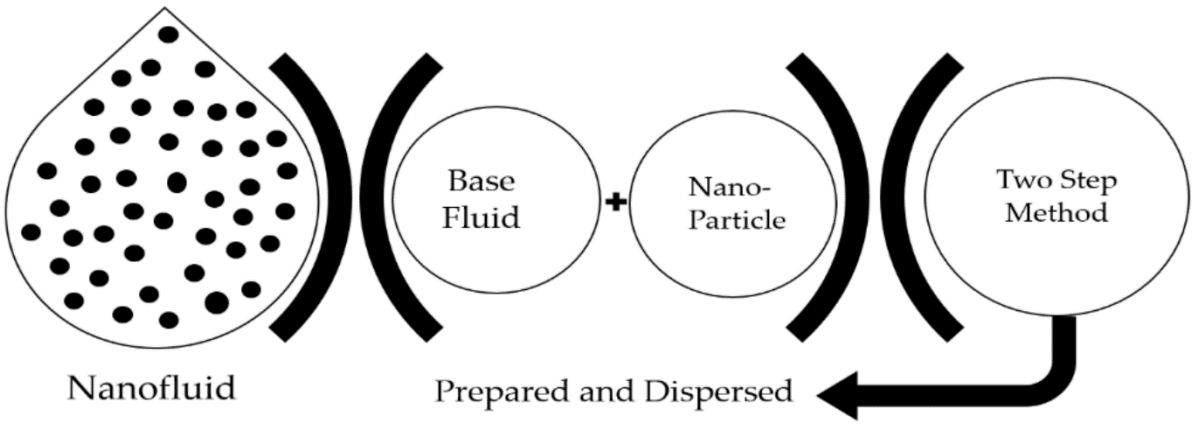

Figure I. 3. Two-Step Method.

I.5 The advantages and the limitations of nanofluids:

I.5.1 Advantages of nano-fluids:

1. Enhanced Thermal Conductivity: Nano-fluids offer increased thermal conductivity, facilitating more efficient heat transfer.

2. Increased Surface Area: Nano-fluids provide a considerable surface area for heat exchange between particles and fluids, improving overall heat transfer efficiency.

3. Reduced Risk of Clogging: Nano-fluids pose less risk of clogging compared to conventional sludge, allowing for smaller system sizes and easier maintenance.

4. Customizable Properties: Properties such as thermal conductivity and surface wettability can be tailored by adjusting particle concentrations, making nano-fluids adaptable to various applications.

5. Focus of Future Studies: Future research should concentrate on material selection, nanoparticle form, and size optimization to maximize thermal conductivity while mitigating viscosity increase

I.5.2 The limitations of nanofluids:

- Nanofluid production often incurs high costs
- The underlying mechanisms driving nanofluid property changes remain inadequately comprehended theoretically.
- The process of manufacturing nanofluids can encounter various technical obstacles.
- Precisely characterizing nanofluid suspensions poses challenges.
- Maintaining stable dispersion of nanoparticles within the fluid presents a significant challenge.
- Utilizing nanofluids may result in higher pressure drop and pumping power demands.
- Nanofluids, due to nanoparticle inclusion, exhibit increased viscosity and reduced specific heat capacity.

I.5.3 Risks

- Toxicity of Nanoparticles: Some nanoparticles used in nanofluids can be toxic to human health and the environment. It is essential to take appropriate precautions during the handling and disposal of nanofluids to minimize the risks of exposure.
- Environmental Impact: Nanoparticles can have adverse effects on the environment, especially if they are released into aquatic or terrestrial

ecosystems. Thorough studies are needed to assess the environmental impact of nanofluids.

- Interaction with Materials: Nanofluids can interact with the materials of the systems in which they are used, which can lead to corrosion.

I.6 Field of applications of nanofluids:

The combination Because of their enhanced heat transfer and thermal conductivity qualities, nanofluids have a broad range of applications in several industries. The following are some areas where nanofluids are used.

1. Electronic cooling: By more effectively dispersing heat, nanofluidscanbe employed to enhance the cooling of electronic components like chips and CPUs.

2. The automobile industry: By using nanofluids as coolants in engine cooling systems, automobile manufacturers may increase thermal efficiency and enhance temperature control.

3. Renewable energies: Heat exchangers in geothermal power plants and solar thermal systems can both benefit from the use of nanofluids to improve heat collection and storage efficiency.

4. Medical uses: Cryotherapy and the cooling of medical equipment, such as magnetic resonance imaging (MRI) machines, are two uses for nanofluids**.**

5. Industrial cooling: By using nanofluids to cool manufacturing processes and industrial facilities, heat exchange efficiency can be increased.

6. Warm capacity:Nanofluids can be utilized in warm capacity frameworks to progress the capacity and productivity of warming and discuss conditioning frameworks.

7. Space applications: Nanofluids can be utilized for the cooling of space hardware, where warm administration is significant due to the extraordinary conditions of space.

8. Power electronics: Power electronics parts like batteries and power converters can have better cooling thanks to the use of nanofluids.

9. Oil and gas field: Nanofluids can be connected to move forward warm exchanges in gear utilized within the investigation and generation of hydrocarbons.

10. Environmental applications: Water purification, desalination, and wastewater treatment are among the uses for nanofluids.

I.7 Dimensionless numbers

I.7.1 Nusselt number

The Nusselt number is a dimensionless quantity used in thermodynamics to characterize heat transfer. It is defined as the ratio of convective heat transfer to conductive heat transfer across a fluid boundary layer.

$$\mathrm{Nu} = \frac{hl}{\lambda}$$

h: Convective heat transfer coefficient.

L: Characteristic length.

λ: Thermal conductivity of the fluid.

I.7.2 Rayleigh number

The Rayleigh number (Ra) is a dimensionless quantity that plays a role in thermal convection phenomena, particularly in fluids. It characterizes the ratio between the effects of natural convection (due to thermal density differences) and thermal conduction in a fluid.

The general formula for the Rayleigh number can be expressed as follows:

$$\boldsymbol{Ra} = \frac{\boldsymbol{g\beta L^3 \Delta T}}{\boldsymbol{\alpha v}}$$

Where:

g: Acceleration due to gravity.

β: Volumetric expansion coefficient.

ΔT: Temperature difference between the walls.

L: Height of the fluid layer.

ν: Kinematic viscosity.

α: Thermal diffusivity.

I.7.3 Hartmann number

The Hartmann number is often used to characterize the importance of magnetic forces compared to viscous forces in an electrically conductive fluid subjected to a magnetic field. It is particularly relevant in applications related to magnetohydrodynamics.

The Hartmann number, denoted as Ha, is defined as:

$$Ha = B_0 L \sqrt{\frac{\sigma}{\rho \upsilon}}$$

Where:

B: Magnetic induction.

L: Characteristic length.

σ: Electrical conductivity of the fluid.

ρ: Fluid density.

ν: Kinematic viscosity.

Chapter II : Governing Equations and Problem Formulation

Chapter II Governing equations and problem formulation

II.1.Introduction

The study of physical phenomena necessitates formalizing the governing laws into mathematical equations and establishing connections among the involved variables. Typically, these fundamental equations manifest in several forms.

Firstly, the continuity equation embodies the principle of mass conservation, illustrating how the total mass within a system remains constant over time, albeit subject to redistribution or transformation.

Next, the Navier-Stokes equations become integral, embodying the conservation of momentum. These equations are pivotal in elucidating fluid dynamics concerning pressures, viscosities, and external forces.

Finally, the energy equation assumes centrality, expressing the conservation of energy within the system under study. This equation delineates energy transfer, storage, and dissipation, crucial for comprehending temperature variations and heat flows.

Concurrently, delineating a problem necessitates specifying boundary conditions, defining behaviors or variable values at the study field's periphery. Moreover, in stationary processes, initial conditions must be established to delineate the system's state at a given initial moment.

In essence, the mathematical formalization of physical laws, augmented by boundary and initial conditions, constitutes a fundamental framework for analyzing and resolving complex physical problems.

II.2.Geometric shape

A schematic diagram of the partially heated enclosure is presented in Figure II.1The enclosure's fluid is a water-based nanofluid that contains many nanoparticle types, including Cu, Al2O3. The flow is taken to be laminar and the nanofluid to be incompressible. It is assumed that there is no slippage between the nanoparticles and the base fluid, which is water, and that they are in a state of thermal equilibrium. Table II.1 provides the nanofluids thermophysical characteristics. A consistent temperature (TH) greater than the right wall (TL) is maintained for the left wall. With the exception of the density fluctuation,which is estimatedvia the Boussinesq model, the thermo-physical characteristics of the nanofluid are taken to be constant.

Table II. 1. Thermophysical propertiesoffluid and nanoparticles.

Physical properties	Fluid phase (water)	Cu	Al_2O_3
C_p(J/kgK)	4179	385	765
ρ (kg/m^3)	997.1	8933	3970
K (W/mK)	0.613	400	40
a × 10^7 (m^2/s)	1.47	1163.1	131.7
b × 10^{-5} (1/K)	21	1.67	0.85

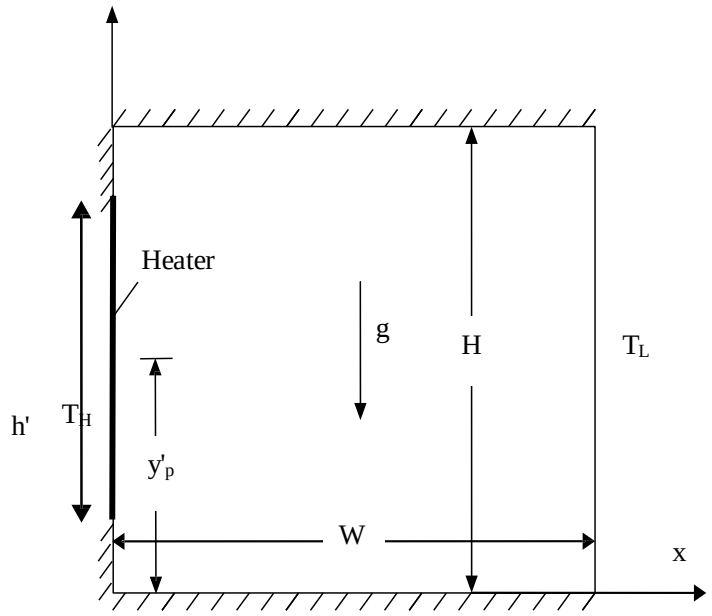

Figure II. 1. Sketch of the coordinates and geometry of the problem.

According to the stream function-vorticity formula, the governing equations for laminar and steady state natural convection are

Vorticity

$$\frac{\partial}{\partial x'}\left(\omega\frac{\partial \psi}{\partial y'}\right)-\frac{\partial}{\partial y'}\left(\omega\frac{\partial \psi}{\partial x'}\right) = \frac{\mu_{nf}}{\rho_{nf}}\left(\frac{\partial \omega}{\partial x'^2}+\frac{\partial \omega}{\partial y'^2}\right)+\frac{(\varphi\rho_s\beta_s+(1-\varphi)\rho_f\beta_{f\gamma})}{\rho_{nf}}\boldsymbol{g}\left(\frac{\partial T}{\partial x'}\right) \quad \textbf{(II.1)}$$

Energy

$$\frac{\partial}{\partial x'}\left(T\frac{\partial \psi}{\partial y'}\right)-\frac{\partial}{\partial y'}\left(T\frac{\partial \psi}{\partial x'}\right)=\frac{\partial}{\partial x'}\left[\alpha_{nf}\frac{\partial T}{\partial x'}\right]+\frac{\partial}{\partial y'}\left[\alpha_{nf}\frac{\partial T}{\partial y'}\right] \quad \textbf{(II.2)}$$

Kinematics

$$\frac{\partial^2 \psi}{\partial x'^2}+\frac{\partial^2 \psi}{\partial y'^2}=-\omega \quad \textbf{(II.3)}$$

$$\alpha_{nf}=\frac{K_{eff}}{(\rho c_p)_{nf}} \quad \textbf{(II.4)}$$

Table II. 2. Properties de nanofluidsdeSheikholeslami et al. [24].

Thermophysical property	Relation
Density	$\rho_{nf}=(1-\phi)\rho_f+\phi\rho_P$
Dynamic viscosity	$\mu_{nf}=\frac{\mu_f}{(1-\phi)^{2.5}}$
Heat capacity	$(\rho C_p)_{nf}=(1-\phi)(\rho C_p)_f+\phi(\rho C_p)_P$
Expansion coefficient	$(\rho\beta)_{nf}=(1-\phi)(\rho\beta)_f+\phi(\rho\beta)_P$
Diffusivity	$\alpha_{nf}=k_{nf}/(\rho C_p)_{nf}$
Conductivity	$k_{nf}=k_f\left[\frac{(k_f+2k_f)-2\phi(k_f-k_p)}{(k_p+2k_f)+\phi(k_f-k_p)}\right]$

II.3.Equations of transport

When the simplification assumptions are applied, the governing equations can be expressed as follows in dimensional form:

- **General equation of Navier-Stokes**

Here is the equation of Navier-Stokes, and how it is analogous to "**Sum of forces = m a**" for a fluid:

$$\left(\frac{\partial p}{\partial t}+\vec{\nabla}.(\rho\vec{V})\right)+\left(\frac{\partial \rho\vec{v}}{\partial t}+\rho(\vec{V}.\vec{\nabla})\vec{V}\right)=-\vec{\nabla}(p)+\mu\vec{\nabla}^2\vec{V}+\vec{F} \quad \textbf{(II.5)}$$

the mass conservation equation $(\frac{\partial \rho}{\partial t}+\nabla.(\rho V)=0.$

Momentum equation $\left(\frac{\partial \rho\vec{V}}{\partial t}+\rho(\vec{V}.\vec{\nabla})\vec{V}\right)=-\vec{\nabla}_{(P)}+\mu\vec{\nabla}^2\vec{V}+\vec{F}$

We apply the simplification assumptions, the governing equations can be

written in dimensionless form as follows :

- **Continuity equation :**

$$\frac{\partial U}{\partial X}+\frac{\partial V}{\partial Y}=0 \quad \textbf{(II.6)}$$

- **Momentumequation :**

Axial:

$$U\frac{\partial U}{\partial X}+V\frac{\partial V}{\partial Y}=\frac{1}{\rho_{nf}}\left[-\frac{\partial P}{\partial X}+\mu_{nf}\left(\frac{\partial^2 U}{\partial X^2}+\frac{\partial^2 U}{\partial Y^2}\right)\right] \quad \textbf{(II.7)}$$

Vertical:

$$U\frac{\partial U}{\partial X}+V\frac{\partial V}{\partial Y}=\frac{1}{\rho_{nf}}\left[-\frac{\partial P}{\partial X}+\mu_{nf}\left(\frac{\partial^2 V}{\partial X^2}+\frac{\partial^2 V}{\partial Y^2}\right)+(\rho\beta)_{nf}g(T-Tc)\right]+\sigma_{nf}{B_0}^2\nu \quad \textbf{(II.8)}$$

- **Energy equation:**

$$U\frac{\partial T}{\partial X}+V\frac{\partial T}{\partial Y}=\alpha_{nf}\left[\frac{\partial^2 T}{\partial X^2}+\frac{\partial^2 T}{\partial Y^2}\right] \quad \textbf{(II.9)}$$

This equation can only be used to spherical nanoparticles; it cannot be used for other nanoparticle shapes. According to research on heat transfer increase with nanofluids, this model is suitable (Akbarinia and Behzadmehr, 2007; Abu-Nada, 2008; Palm et al., 2006; Maiga et al., 2005).According to Brinkman (1952), the viscosity of the nanofluid is about equal to the viscosity of a base fluid containing a diluted suspension of tiny spherical particles.

$$\mu_{nf}=\frac{\mu_f}{(1-\varphi)^{2,5}} \quad \textbf{(II.10)}$$

The radial and tangential velocities are given by the following relations respectively

$$u=\frac{\partial \psi}{\partial y'} \quad \textbf{(II.11)}$$

$$v=-\frac{\partial \psi}{\partial x'} \quad \textbf{(II.12)}$$

The following dimensionless groups are introduced

$$x=\frac{x'}{H}y=\frac{y'}{H};\ \Omega=\frac{\omega H^2}{\alpha_f};\Psi=\frac{\psi}{\alpha_f};V=\frac{vH}{\alpha_f}U=\frac{uH}{\alpha_f};\theta=\frac{T-T_L}{T_H-T_L}; \quad \textbf{(II.13)}$$

By using the dimensionless parameters the equations are written as

$$\frac{\partial}{\partial x}\left(\Omega\frac{\partial \Psi}{\partial y}\right)-\frac{\partial}{\partial y}\left(\Omega\frac{\partial \Psi}{\partial x}\right) = \left[\frac{Pr}{(1-\varphi)^{0.25}\left((1-\varphi)+\varphi\frac{\rho_s}{\rho_f}\right)}\right]\left(\frac{\partial \Omega}{\partial x^2}+\frac{\partial \Omega}{\partial y^2}\right) + R_a P_r\left[\frac{1}{\frac{(1-\varphi)}{\varphi}\frac{\rho_f}{\rho_s}+1}\frac{\beta_s}{\beta_f}+\frac{1}{\frac{\varphi}{(1-\varphi)}\frac{\rho_f}{\rho_s}+1}\right]\left(\frac{\partial T}{\partial x}\right) \quad \textbf{(II.14)}$$

$$\frac{\partial}{\partial x}\left(\theta\frac{\partial \Psi}{\partial y}\right)-\frac{\partial}{\partial y}\left(\theta\frac{\partial \Psi}{\partial x}\right)=\frac{\partial}{\partial x}\left(\lambda\frac{\partial \theta}{\partial x}\right)+\frac{\partial}{\partial y}\left(\lambda\frac{\partial \theta}{\partial y}\right) \quad \textbf{(II.15)}$$

$$\frac{\partial^2 \Psi}{\partial x^2}+\frac{\partial^2 \Psi}{\partial y^2}=-\Omega \quad \textbf{(II.16)}$$

$$\lambda=\frac{\frac{K_{nf}}{K_f}}{(1-\varphi)+\varphi\frac{(\rho c_P)_s}{(\rho c_P)_f}} \quad \textbf{(II.17)}$$

$$Ra=\frac{g\beta H^2(T_H-T_L)}{v\alpha} \quad \textbf{(II.18)}$$

The dimensionless radial and tangential velocities are given as, respectively:

, $$U=\frac{\partial \Psi}{\partial y} \quad \textbf{(II.19)}$$

$$V=-\frac{\partial \Psi}{\partial x}, \quad \textbf{(II.20)}$$

The dimensionless boundary conditions are written as

1- On the left wall (heater)i.e., $x=0,\ \Psi=0, \Omega=-\frac{\partial^2 \Psi}{\partial x^2}, \theta=1.$

2- On the left wall (no heater)i.e., $x=0,\ \Psi=0, \Omega=-\frac{\partial^2 \Psi}{\partial x^2}, \frac{\partial \theta}{\partial x}=0.$

3- On the right wall i.e., $x=1,\ \Psi=0, \Omega=-\frac{\partial^2 \Psi}{\partial x^2}, \theta=0.$

4- On the top and bottom wall :$\Psi=0,, \Omega=-\frac{\partial^2 \Psi}{\partial y^2}, \frac{\partial \theta}{\partial y}=0.$

(II. 21)

The equations (II.2-6) can be converted to the dimensionless form presented by Eq (II.7)

$$\frac{\partial (U_\varphi)}{\partial X}+\frac{\partial (V_\varphi)}{\partial Y}=\frac{\partial}{\partial X}\left(\Gamma_\varphi\frac{\sigma_{(\varphi)}}{\partial X}\right)+\frac{\partial}{\partial Y}\left(\Gamma_\varphi\frac{\sigma_{(\varphi)}}{\partial Y}\right)+S_\varphi \quad \textbf{(II.22)}$$

Where represents the dimensionless parameters dependent on U, V, and , are the corresponding diffusion and source terms, respectively, as summarized in Table (II.3).

Table II. 3. Summary of the two-dimensional fundamental equations.

Equation	φ	Γ_φ	S_φ
Continuity	1	O	
X-Movement	U	$\frac{\mu_{nf}}{\rho_{nf}\nu_{nf}}$	$-\frac{\partial P}{\partial X}$
Y-Movement	V	$\frac{\mu_{nf}}{\rho_{nf}\nu_{nf}}$	$-\frac{\partial P}{\partial Y}+\frac{(\rho\beta)_{nf}}{\rho_{nf}\beta_f}RaPr\theta - Ha^2PrV$

The local and mean Nusselt numbers define heat transfer and the mode of convection are expressed as follows:

$$\boldsymbol{Nu(Y) = -\frac{k_{nf}}{k_f}|_{X=0}\ \text{and}\ Numoy = \int_0^1 Nu(Y)dY} \qquad \textbf{(II.23)}$$

The influence of the applied magnetic field on the swirling of the nanofluid flow results in an electric current density J, in accordance with Ohm's law as described by [25].

$$\boldsymbol{J = \sigma_{nf}(E + V \times B)} \qquad \textbf{(II.24)}$$

Where V is the velocity vector (u, w, v), E is the electric field, and the applied magnetic field is B(0, 0, B_0).

The law of Faraday for the magnetic field gives

$$\boldsymbol{\nabla \times E = 0} \qquad \textbf{(II.25)}$$

This means that the electric potential is

$$\boldsymbol{E = -\nabla\phi} \qquad \textbf{(II.26)}$$

Conservation of electric current leads to:

$$\boldsymbol{\nabla J = 0} \qquad \textbf{(II.27)}$$

In other words, the electric current results from an electric potential Φ. By replacing equations (7) and (8) into equation (6), we obtain:

$$\boldsymbol{\nabla.\left(\nabla_\varphi + V \wedge B\right) = 0 \ \ll=\gg \ \ \nabla\phi = \nabla(V \wedge B)} \qquad \textbf{(II.28)}$$

As a result, the Laplace equation for the electric potential becomes

$$\mathbf{1}\, r\partial\partial(r\ \partial\phi\ \partial r) + \frac{\sigma^2\phi}{\partial r^2} = \mathbf{0} \qquad \textbf{(II.29)}$$

When assuming the existence of a constant and uniform magnetic field directed vertically through the cylinder, this suggests that the Lorentz force depends only on the variables (r) and (θ).

They can be found by: $F_L = J \times B$, the dimensionless Lorentz forces in the x, y directions are respectively

II.4.Conclusion

This section introduces the physical model under investigation and the equations governing the phenomenon in question. Below, we have outlined the restrictions that apply to the entire border of this domain.

Chapter III : Numerical implementation and Grid testing

Chapter III. Numerical implementation and Grid testing

III.1.Introduction

In order to model and simulate complicated mathematical and physical phenomena, one essential step in the process is the digital resolution of equations with partial derivatives (PDEs). Among the often-used discretization methods, the Finite Volume Method (FVM) stands out for its ability to offer precise and stable solutions for a wide range of issues. This report provides a detailed exploration of the Finite Volume Method (FVM) as a discretization method, including its underlying principles, implementation methodology, and its role in identifying variable fields in a given problem.

III.2.Fundamental principle of the finite volume method

One popular method of discretization for solving PDEs is the Finite Volume Method. Its basic idea is to discretize space into closed volumes, often called cells or mesh elements. Instead of solving equations at individual points, the FVM focuses on integrating the equations over each finite volume surrounding a mesh point. This integration over finite volumes makes it possible to account for the flow entering and exiting cells across their borders, which is crucial for accurately modeling transport, diffusion, and convection phenomena.

III.3.Putting the method of final volumes into practice

There are various steps involved in putting the Finite Volume Method into practice. Firstly, the computational domain is divided into a mesh composed of small cells. Subsequently, each cell encompasses the partial equations of the problem, taking into account flows, boundary conditions, and source terms. The values of the unknown variables are then estimated at the center of each cell, and the discretized equations are assembled to form a linear system of equations. Solving this system of equations allows determining the values of unknown variables throughout the entire computational domain. The FVM offers considerable flexibility in choosing numerical schemes to approximate spatial and temporal derivatives, enabling adaptation of the method to the specific characteristics of the problem.

III.4.The method of final volumes: advances and applications

There are various benefits associated with the Finite Volume Method. It is particularly well-suited for complex geometries and non-structured meshes, making it a popular choice for

a variety of applications including fluid mechanics, thermodynamics, electromagnetics, heat diffusion, and many more. Additionally, the FVM ensures physically coherent results by preserving attributes such as mass, energy, and momentum.

In summary, the Finite Volume Method provides a robust and versatile approach for the numerical solution of partial differential equations. Its accurate modeling of a wide range of physical phenomena is enabled by its volume-based spatial discretization principle combined with appropriate numerical schemes. The FVM is widely employed across various scientific and engineering disciplines, significantly enhancing the understanding and resolution of complex problems.

To illustrate the use of this method, consider the general transport equation written for a property Φ as follows:

$$\frac{\partial \rho \Phi}{\partial t} + \text{div}\,(\rho \Phi u) = \text{div}\,(\Gamma_\Phi \text{grad}\Phi) + S_\Phi$$

Stated differently:

$$(\text{Variation of } \Phi \text{ in a fluid element}) + \underbrace{(\text{net flow of a fluid element})}_{convective\ term}$$
$$= \underbrace{(\text{variation in } \Phi \text{ as a result of diffusion})}_{diffusive\ term}$$
$$+ \underbrace{(\text{change in } \Phi \text{ due to the sources})}_{source\ term}$$

Such as :

Γ_Φ : the diffusion coefficient.

S_Φ:the source term.

The primary step in solving the equation using the finite volume method is integrating it over a control volume.

$$\int_{cv} \frac{\partial(\rho\Phi)}{\partial t} dv + \int_{cv} \text{div}\,(\rho \Phi u) dv = \int_{cv} \text{div}(\Gamma_\Phi \text{grad}\Phi)\, dv + \int_{cv} S_\Phi\, dv$$

III.5.Resolution peaks using the method of final volumes

1. Domain discretization: Divide your calculation domain into a discrete cell mesh. These cells form a set of finite volumes on which the equation will be solved. Each cell shares common boundaries with its neighboring cells.

2. Discrete equivalence: For each cell in the mesh, modify the transport equation by substituting appropriate approximations for the partial derivatives. For example, methods like finite elements or finite differences can be used to approximate the spatial derivatives. This results in a discrete equation for each cell.

3. Volume integration: Integrate the discrete equation over each cell to derive a volume equation specific to that cell. This involves integrating the terms over the internal part of the cell as well as accounting for the flow through its faces.

4. Estimation of flow: The flow through each cell's faces needs to be approximated. Depending on the geometry of the mesh and the expected solution, this can be achieved using suitable numerical schemes such as centered flux schemes or upwind flux schemes.

5. Compilation of local equations: By combining the derived balance equations for each cell, you form a system of linear equations that covers the entire domain. This structure will include significant variations in the values of Φ across each cell.

6. Boundary conditions: Incorporate the relevant boundary conditions into the equation system. These conditions may specify values at domain boundaries or particular internal conditions within the domain.

7. Solution of the system of equations: Solve the resulting linear equation system to find the values of Φ that satisfy the equations within each mesh cell. This can be achieved using numerical techniques such as iterative methods (e.g., Gauss-Seidel method) or direct methods (e.g., LU decomposition method).

8. Calculate the numerical flux: Once the values of Φ for each cell have been determined, use the approximate values of the spatial derivatives to compute the numerical flux across the faces of the mesh.

9. Temporal discretization: If the problem evolves over time, employ a temporal discretization scheme (such as explicit or implicit methods) to update the values of Φ over time.

10. Temporal iterations: To monitor the evolution of Φ over time, repeat steps 2 through 9 for each time step.

These steps outline the complete process of solving the transport equation using the Finite Volume Method. The level of detail can vary depending on choices regarding numerical schemes, integration methods, boundary conditions, etc.

III.6.Mesh

The calculation domain is divided into control volumes that collectively cover the entire domain, ensuring their volumes sum up to the total volume of the domain. The dimensionless governing equations with boundary conditions are solved using the finite volume method, employing Patankar's SIMPLE algorithm. Convection-diffusion terms are discretized using a power-law scheme, and the simulation is performed using Fluent (student version).

The solution domain is represented by a two-dimensional staggered grid with uniform spacing. Grid independence is assessed in this study, and results presented in Fig. III.1 indicate that a grid size of 50 × 50 satisfies the grid independence criterion. Convergence ismonitored by reducing the maximum residual mass of the control volume grid below 10^{-6}

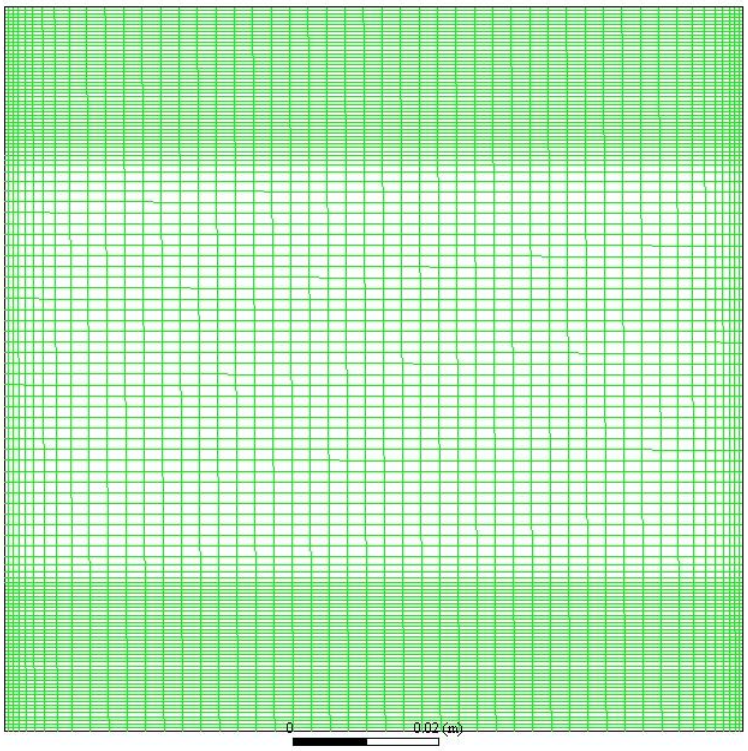

Figure III.1. Mesh (50×50 nodes).

• Relationship between velocity and pressure:

The equations governing momentum components are interconnected because pressure influences them through pressure gradients. However, there is no separate equation that directly describes pressure as an independent variable.

• Algorithm Used:

The algorithm used is the SIMPLE algorithm, which stands for "Semi-Implicit Method for Pressure Linked Equations." This method is employed to solve the system of discretized equations, establishing a relationship between corrected velocities and pressures to ensure mass conservation during the solution process.

When discrediting a transport-diffusion equation over a control volume using the finite volume method, the velocities at volume interfaces (Ue, Uw, Us, Un) are crucial. Directly calculating these velocities at the interfaces offers advantages by avoiding additional interpolations.

To address issues such as "checkerboard" distributions of pressure or velocity, which can lead to significant errors when using linear interpolation for discretizing the continuity equation and pressure gradients, staggered grids are preferred. In this approach, a main grid computes pressure, temperature, and concentration, while two additional staggered grids, shifted horizontally and vertically, handle horizontal and vertical velocities.

The solution of these discretized equations utilizes the SIMPLE algorithm, which ensures mass conservation is maintained throughout the solution process by establishing a relationship between corrected velocities and pressures.

III.7. Numerical parameters used in this study:

FLUENT employs the finite volume method for discretizing and solving the equations governing flow, including the continuity equation, momentum equation, and energy equation. This method integrates these equations over defined control volumes. FLUENT software provides a user-friendly graphical interface, allowing both standard and advanced users to utilize its capabilities. Advanced users can further customize the interface through macros and menu functions to automate specific procedures as required. The discretization schemes used

for different variables are summarized in the following table: [Table summarizing discretization schemes for various variables].

Table III. 1. Discretization Schema.

Variable	Scheme
The pressure	Standard Scheme
Eq.Amount of movement	Upstream offset (1st order)
Eq.Energy	Upstream offset (1st order)
Pressure-velocitycoupling	Simple Algorithm

• Under-Relaxation:

In our case, the values of under-relaxation are summarized in the following table. Under-relaxation is commonly used in solving nonlinear problems to prevent the divergence of iterative processes. It involves introducing a relaxation coefficient to moderate the rate of variable fluctuations between iterations.

Table III.2. Under-relaxation factors.

Factors that contribute to sublimation	Variable
0.3	Pressure
0.7	Amount of movement
1	Density
1	Energy

• Convergence criteria:

Convergence is achieved when errors decrease over iterations until they reach a specified tolerance ε. A procedure is considered convergent when further iterations do not lead to significant changes in the variables, as defined by a user-defined criterion. Throughout our study, the convergence criterion is set at a normalized residual value less than or equal to 10^6

Conclusion:

This chapter provides a brief introduction, an overview of the finite volume method, and details on the numerical parameters utilized in this study. The results obtained from the simulations conducted using FLUENT software will be presented in the next chapter.

Chapter IV: Results and discussion

Chapter IV: Results and Discussion

IV.1 Introduction

This study numerically investigates the natural convection in a square container filled with a nanofluid consisting of water- Al2O3, water-copper, and subjected to the influence of a horizontally applied magnetic field. Natural convection is checked in a square container filled with a nanofluid consisting of water- Al2O3, water-copper, and is affected by a magnetic field. The effects of parameters such as Rayleigh number, solid volume fraction, and Hartmann number on the flow and temperature fields, as well as the heat transfer rate were examined.

IV.2 Mesh independence test

Given the coupled natural convection with the Hartmann layer, careful mesh selection is necessary to ensure good accuracy. A mesh with quadratic elements has been chosen; details of the mesh independence tests are presented in Table 1. The influence of the number of control volumes on result accuracy has been studied, with the average Nusselt number across the heated wall as a function of solid volume fraction ϕ. As we increase the number of control volumes above 50×50, the average Nusselt number becomes nearly constant. Consequently, a 50×50 node grid was used in all calculations of this study.

Table IV. 1. Mesh Independence Test at $Ra=10^5$.

Grid (x, y)	Numoy ((ϕ =0,0)	Numoy ((ϕ =0.0 3)	Numoy ((ϕ =0.06)
40×40	3.101	3.112	2.989
50×50	**3.155**	**3.134**	**3.103**
60×60	3.144	3.123	3.005
90×90	3.156	3.134	3.105

IV.3.Validation

The numerical code is also validated against the results of other studies relating to convection induced by a magneto-hydrodynamic thrust in enclosures. For example, the results of convective heat transfer in a square enclosure obtained from the current model are validated against the results of the study conducted by Ghassemi et al. [2] (Fig. IV.2). In this study, we examined natural convection in an enclosure filled with a water-Al2O3 nanofluid and influenced by a magnetic field. We investigated the effects of important parameters such

as Rayleigh number, solid density fraction, and Hartmann number on heat transfer. Fig. (VI.3) shows the current function for the case Ra = 10^5 and ϕ = 0.03, where our results are schematized below.

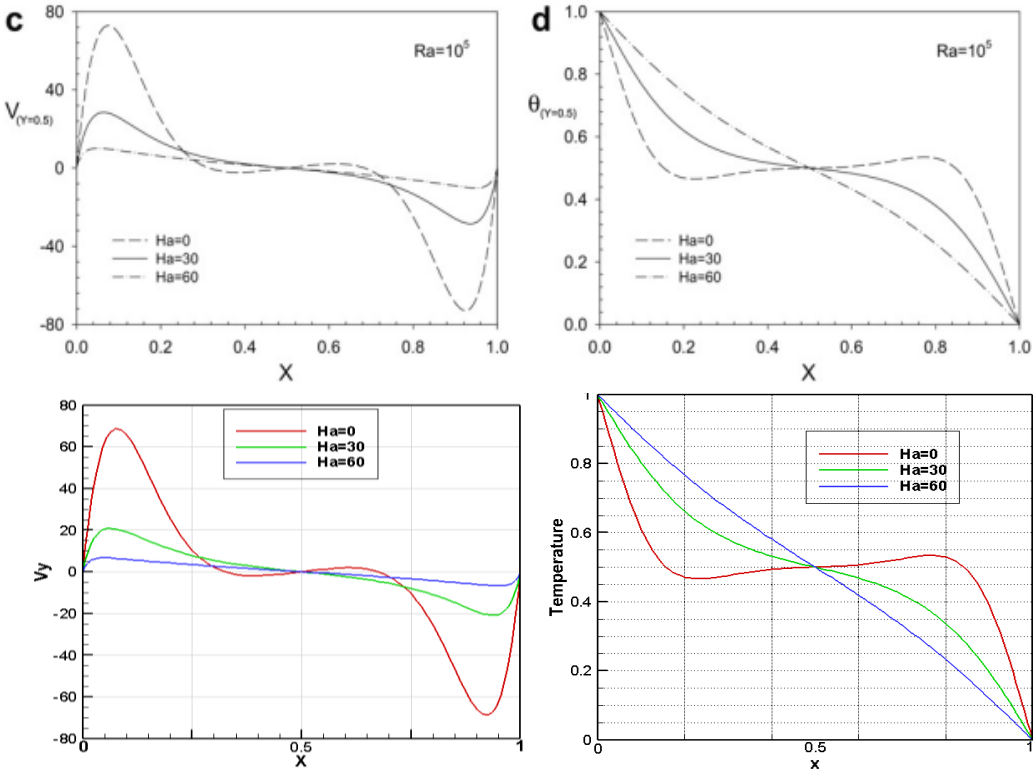

Figure IV. 1. Validation of present results (bottom) with [2] (top) in ϕ= 0.03 and Ra = 10^5.

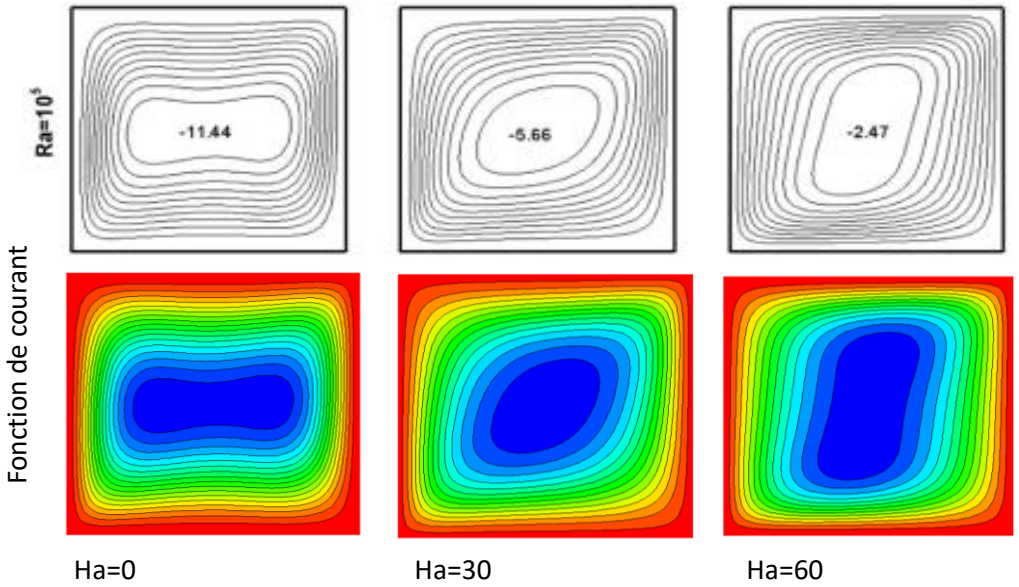

Figure IV. 2. Validation of these results (bottom) with [2] (top) in the case Ra=10^5 and ϕ=0.03.

IV.4 Buoyancy effect on structure flow

a) Cu-water nanofluid case

Utilizing the finite volume method, this study delves into the numerical analysis of buoyancy-induced flow within a partially heated square enclosure filled with nanofluid. Key factors such as the volume fraction of nanofluid, nanoparticle composition, magnetic field presence, and Rayleigh number are meticulously scrutinized. The baseline scenario is a square cavity with dimensions set at h = 0.5 and yp = 0.5, while the Prandtl number remains fixed at Pr = 6.2. In Figure IV.3, we observe the behavior of Cu-water nanofluid on isotherms (upper panel) and streamlines (lower panel) across varying Rayleigh numbers (Ra = 10^4, 10^5, 10^6).The depicted figures unveil a consistent formation of a single circulation cell along the vertical walls, rotating in a clockwise direction. As the Rayleigh number escalates, the length of this cell expands, assuming an egg-shaped contour. Particularly noteworthy is the transformation observed at Ra = 10^6, where the flow intensity amplifies, and boundary layers become more pronounced. Isotherms vividly portray heightened temperature gradients adjacent to the heater and cold wall. At Ra = 10^5, streamlines elongate parallel to the horizontal wall in the absence of nanofluid, while an oval-shaped circulation cell emerges near the right vertical boundary

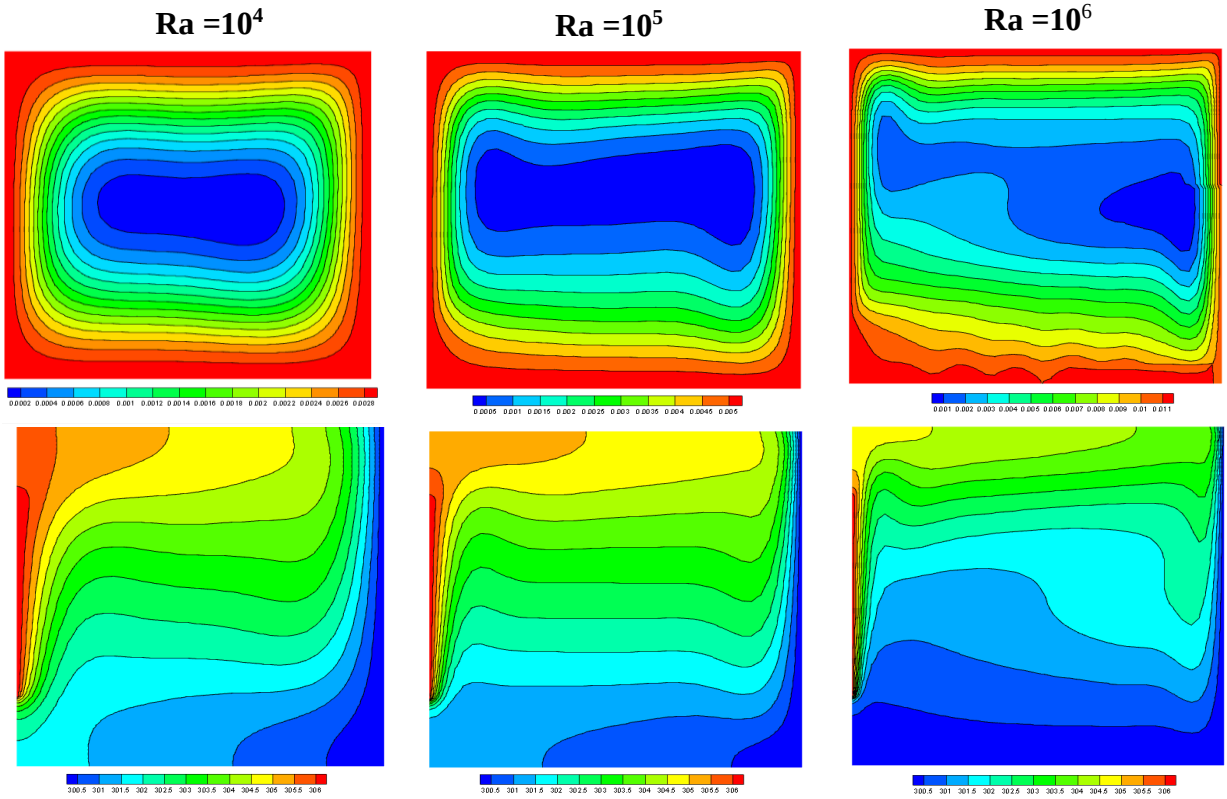

Figure IV. 3. Isotherms (below) and Streamlines (top) for Cu-water nanofluids when Ra =(10^4, 10^5,10^6).

b) Al_2O_3-water nanofluid case

In the study focusing on Al_2O_3-water, akin trends to those observed in Cu-water are discerned. As the Rayleigh number (Ra) escalates, the convection cells undergo a metamorphosis towards increased complexity, consequently enhancing thermal dissipation. Temperature profiles accentuate steeper gradients in proximity to the heated surfaces, while stream functions depict a more dynamic interplay of circulation cells.

Distinct alterations in the maximum temperature near the heated wall are evident across different Rayleigh numbers. At Ra = 10^4, the maximum temperature adjacent to the heated surface registers around 310 K. With a progression to Ra = 10^5, this peak temperature elevates to approximately 320 K, marking a discernible uptick. Further amplification of the Rayleigh number to Ra = 10^6 culminates in the maximum temperature soaring to approximately 330 K. This consistent trend underscores the direct correlation between the Rayleigh number and the thermal dynamics proximate to the heated surface. Higher Rayleigh numbers signify augmented convective heat transfer, consequently manifesting in elevated temperatures

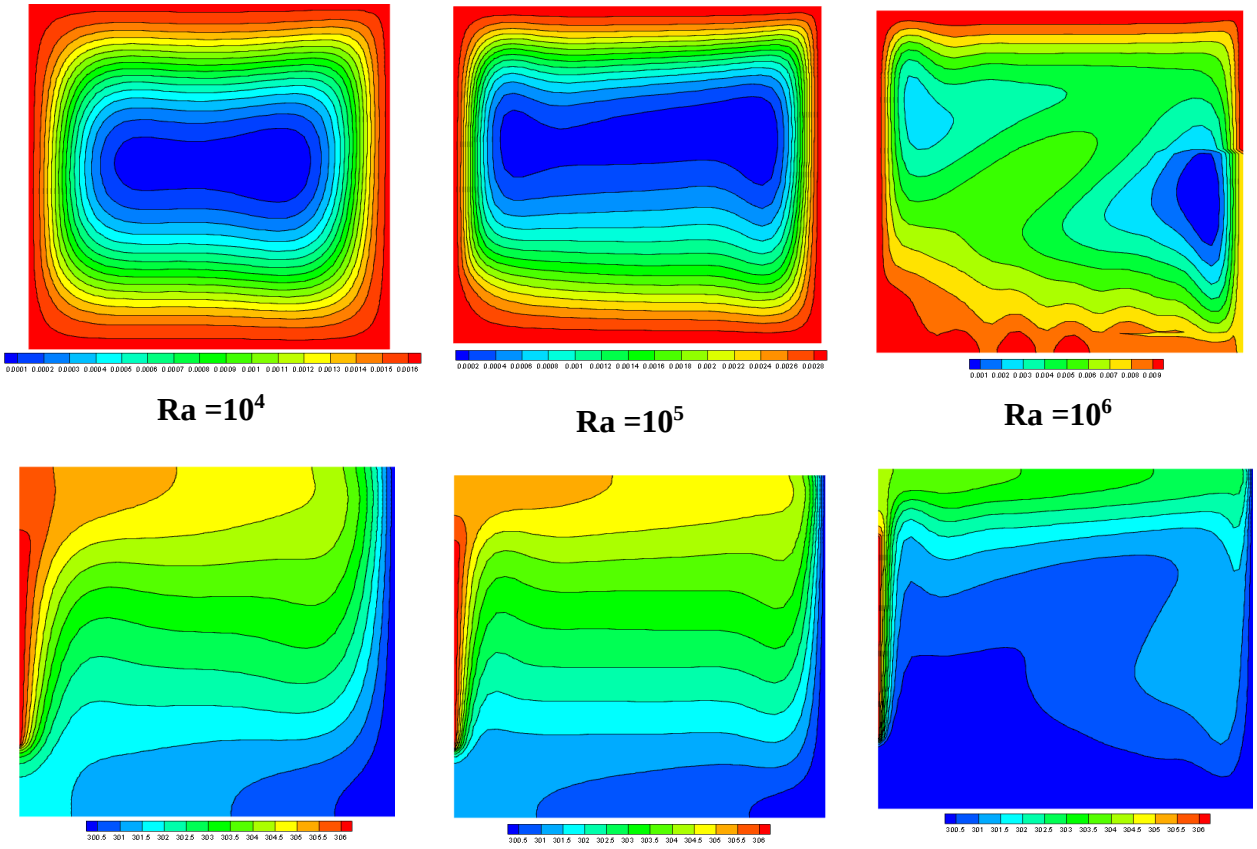

Figure IV. 4. Temperature (below) and streamfunction(top) for Al_2O_3-water nanofluids,Ra =(10^4, 10^5,10^6).

c) Comparison between Cu-water nanofluid and Al_2O_3-water

Illustrated in Fig. VI.5(a)–(c) is a comparative analysis between Cu-water nanofluid (represented by solid lines) and Al_2O_3-water nanofluid (depicted by dashed lines) concerning streamlines (upper portion) and isotherms (lower portion) across varying Rayleigh numbers. Notably, irrespective of the Rayleigh number, a singular circulation cell manifests itself in a clockwise direction.InFig. VI.5(a), depicting Ra = 10^4, a circular-shaped cell emerges with wmin = -4.84. Isotherms corresponding to this scenario exhibit traits indicative of a conduction-dominated regime, aligning approximately parallel to the vertical walls. With the escalation of the Rayleigh number, showcased in Fig. VI.5(b), the circulation cell elongates into an egg-shaped configuration. This augmentation in Rayleigh number corresponds to heightened flow intensity and more distinct boundary layers. Isotherms underscore intensified temperature gradients proximate to both the heater and cold wall.Fig. VI.5(c) delves into Ra = 10^6, wherein streamlines extend parallel to the horizontal wall for the pure fluid. Additionally, an oval-shaped circulation cell materializes adjacent to the right vertical wall, marking a notable departure from preceding configurations.

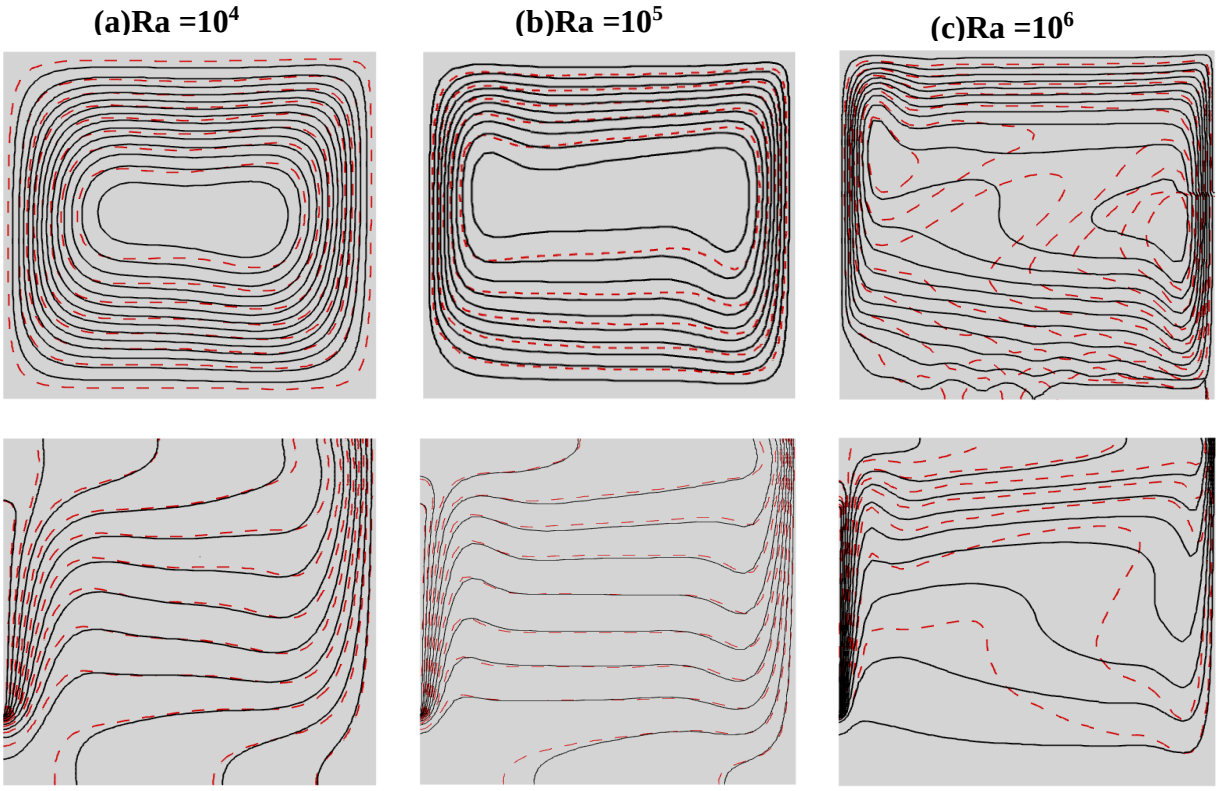

Figure IV. 5. Temperature (on the below) and streamfunction(on the top) for Al2O3-water nanofluids (- - -)with Cu-water nanofluids for (___).

Fig. VI.6(a)–(c), a comprehensive comparison between Cu-water nanofluid and Al_2O_3-water nanofluid is presented, focusing on the vertical velocity profiles at the center of the enclosure. This analysis elucidates the distinct impacts of various nanoparticles—specifically Cu-water and Al_2O_3-water—across different Rayleigh numbers (10^4, 10^5, and 10^6).Given the buoyant flow dynamics within the enclosure, the velocity exhibits a characteristic parabolic variation near the isothermal walls. Interestingly, the vertical velocity appears relatively insensitive to the type of nanoparticles employed, as all three variants exhibit similar vertical velocity distributions. However, a subtle distinction emerges in the maximum vertical velocity, consistently favoring Cu-water over Al_2O_3-water. At Ra = 10^4, Cu-water attains a maximum velocity of approximately 0.02 m/s, slightly surpassing Al_2O_3-water's 0.018 m/s. With an escalation to Ra = 10^5, this disparity widens, with Cu-water peaking at around 0.04 m/s compared to Al_2O_3-water's 0.037 m/s. Subsequently, at Ra = 10^6, Cu-water demonstrates a maximum velocity of approximately 0.06 m/s, while Al_2O_3-water trails slightly behind at 0.055 m/s.These findings underscore Cu-water's marginally superior velocity enhancements across the investigated Rayleigh numbers, underscoring the nuanced influence of nanoparticle selection on fluid dynamics within the enclosure.

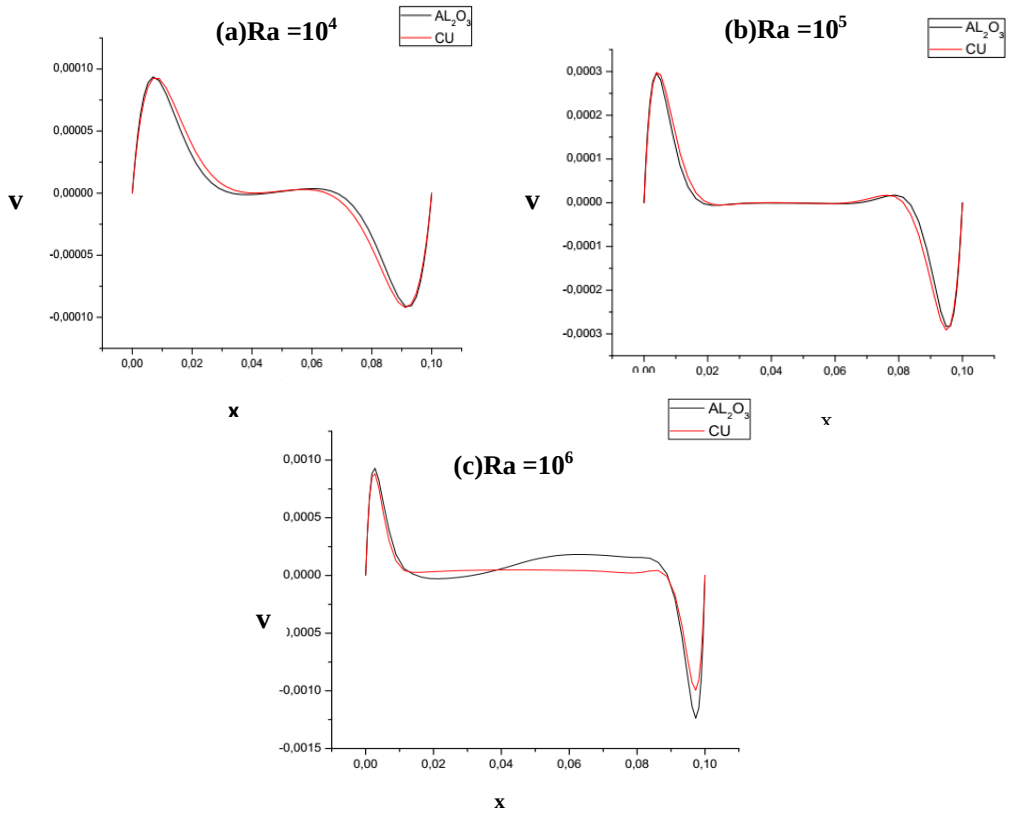

Figure IV. 6. Comparison between Cu-water nanofluid and Al2O3-water nanofluid on the vertical velocity profiles.

d)Heat transfert via nusselt number

Fig. IV.7 illustrates the variation of the local Nusselt number along the partial heater, utilizing different nanoparticles under the parameters specified in Fig. IV.6. Notably, higher local Nusselt number values emerge at the onset and endpoint of the heater, attributable to elevated temperature differentials. The depicted trend unveils an almost U-shaped variation, with Cu nanoparticles yielding the highest local Nusselt number values and pure fluid yielding the lowest.The variation of local Nusselt number with different Rayleigh numbers for Cu-water nanofluid at h = 0.5, yp = 0.5 is portrayed in Fig. IV.7a. Evidently, heat transfer escalates with increasing Rayleigh number, indicative of improved thermal efficiency. Both Al_2O_3 and Cu nanoparticles exhibit a proportional increase in Nusselt number with Rayleigh number, signifying enhanced heat transfer. For Al_2O_3-water nanofluid, the average Nusselt number registers approximately 15 at Ra = 10^4, 20 at Ra = 10^5, and 25 at Ra = 10^6. Conversely, Cu-water nanofluid showcases an average Nusselt number of about 16 at Ra = 10^4, 22 at Ra = 10^5, and 28 at Ra = 10^6.These insights underscore Cu nanoparticles' marginally superior enhancement in heat transfer efficiency compared to Al_2O_3 nanoparticles, with both types exhibiting substantial improvements as Rayleigh number escalates.

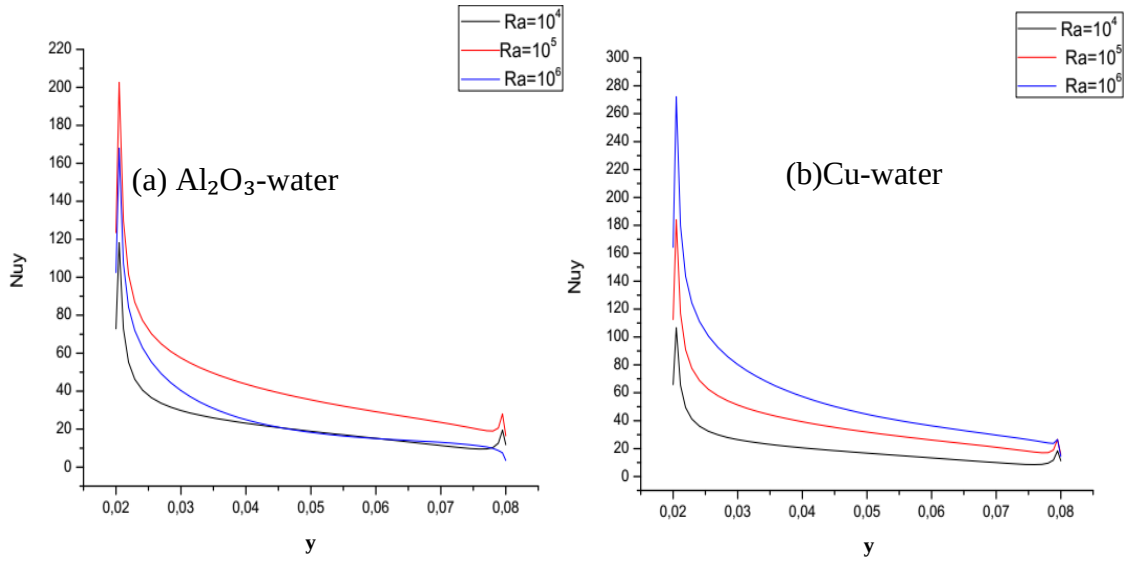

Figure IV. 7. Variation of local Nusselt number along the heated wall(TH)for (a) Al2O3, Cu and (b) Cu-water.

IV.5. Magnetic field effecton flow structure and heat transfer

Studies [6-12] have underscored the potential of magnetic fields in inducing a transition from oscillatory to stable flow, a phenomenon termed electromagnetic stabilization. This mechanism hinges on the generation of electric currents by the movement of electrically conductive fluids within a magnetic field. The interplay between the convective roller and the magnetic field engenders forces capable of modulating flow dynamics. Notably, the formation of a Hartmann layer near walls, induced by the magnetic field, assumes a pivotal role in shaping flow behavior. Such electromagnetic stabilization holds particular significance in systems mandating precise flow control.Fig.IV.8 elucidates the impact of a Cu-water nanofluid under varying Hartmann numbers (Ha), demonstrating a notable attenuation in natural convection intensity as Ha increments to 30 and 60. Observable alterations in isotherms and stream functions accompany this reduction, characterized by diminished temperature gradients and circulation forces. Quantitative assessments corroborate this phenomenon: in the absence of a magnetic field (Ha=0), the maximum temperature approximates 320 K, with a corresponding maximum stream function of approximately 0.015. Upon increasing the magnetic field strength to Ha=30, the maximum temperature diminishes to about 315 K, while the maximum stream function dwindles to roughly 0.012. Further escalation to Ha=60 precipitates a reduction in the maximum temperature to around 310 K, coupled with a significant decrease in the maximum stream function to approximately 0.009. These findings highlight the efficacy of magnetic fields in suppressing natural convection, culminating in lower temperatures and subdued circulation within the system.Similarly, Fig.IV.9 delineates the response of an Al_2O_3-water nanofluid to magnetic field influence, mirroring trends observed in Cu-water. As Ha increases, discernible reductions in temperature gradients and circulation cell intensity ensue. Quantitative analysis reaffirms these trends: absent a magnetic field (Ha=0), the maximum temperature registers approximately 330 K, with a maximum stream function of around 0.016. Application of a magnetic field at Ha=30 prompts the maximum temperature to decline to about 325 K, alongside a reduction in the maximum stream function to approximately 0.013. Further augmentation to Ha=60 elicits a drop in the maximum temperature to roughly 320 K, concomitant with a substantial decline in the maximum stream function to about 0.010. These results underscore the efficacy of increasing magnetic field strength in curtailing natural convection, resulting in diminished temperatures and attenuated circulation within the Al_2O_3-water nanofluid system.

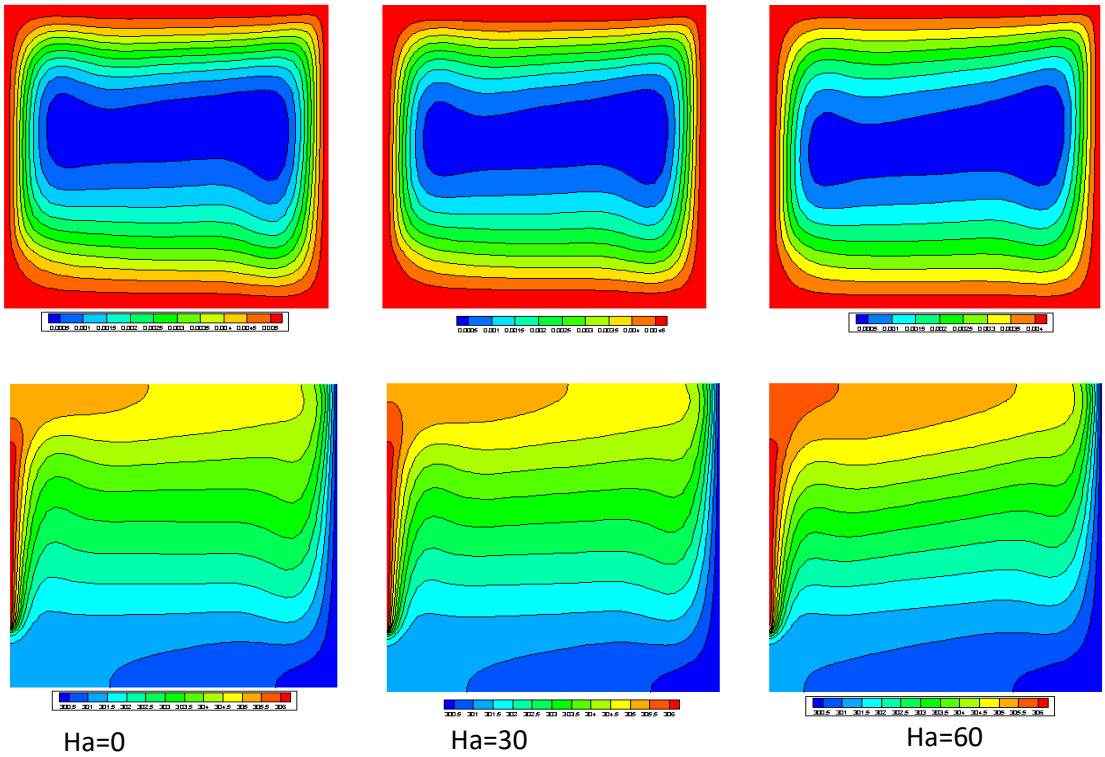

Figure IV. 8. Effect of Magnetic field on Streamlines (on top) and isotherms (on below) of Cu-water nanofluid when Ra =105.

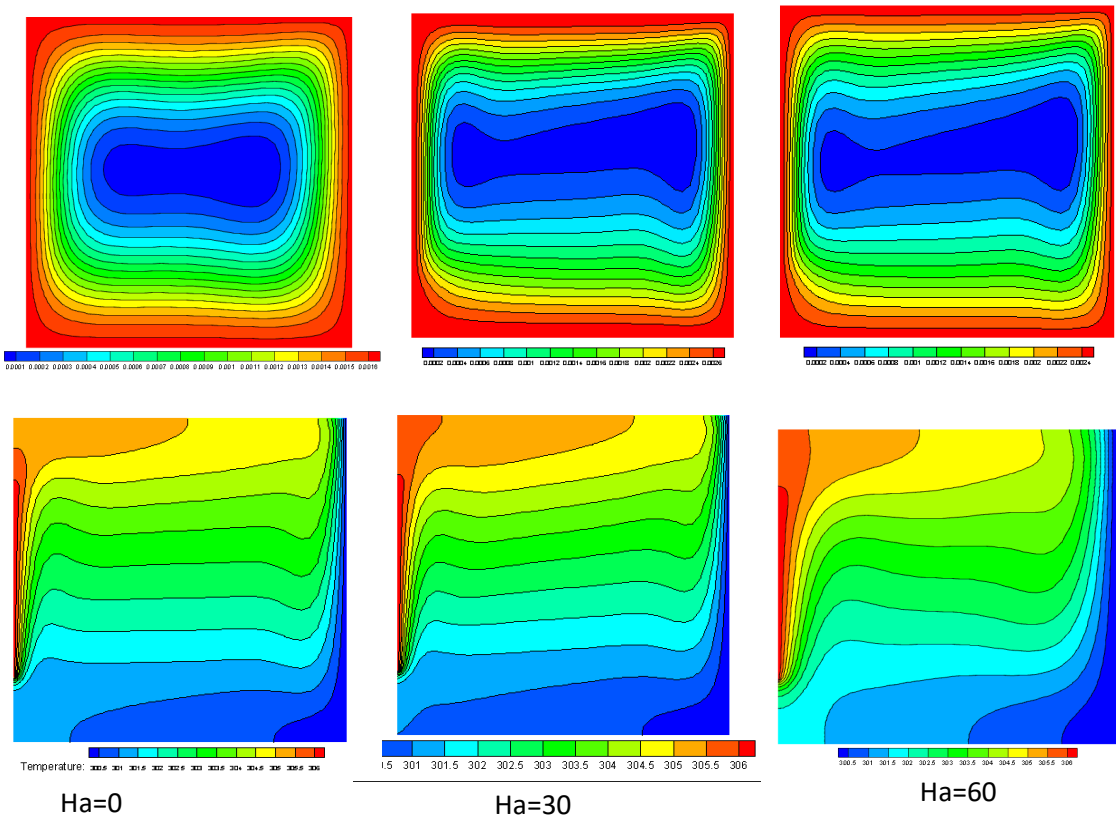

Figure IV. 9. Effect of Magnetic field on Streamlines (on top) and isotherms (on below) of Al_2O_3-water nanofluids when Ra =10^5.

In Fig. (IV.10), a comparative analysis is presented, juxtaposing streamlines and isotherms utilizing different nanofluids—Cu-water and Al_2O_3-water—under varying Hartmann numbers (Ha=0), (Ha=30) and Ha=60) and Rayleigh number (Ra = 10^5). Notably, both nanofluids exhibit a singular circulation cell rotation in a clockwise direction.At lower Hartmann numbers, Al_2O_3-water showcases higher flow strength compared to Cu-water However, an intriguing shift occurs at Ra= 10^5, where the flow strength diminishes for Al_2O_3. Isotherms elucidate subtle disparities in distribution between Al_2O_3-water and Cu-water, particularly noticeable at a high Hartmann number (Ha=60). Under these conditions, both nanofluids tend towards a more conductive flow regime, veering away from convective patterns.

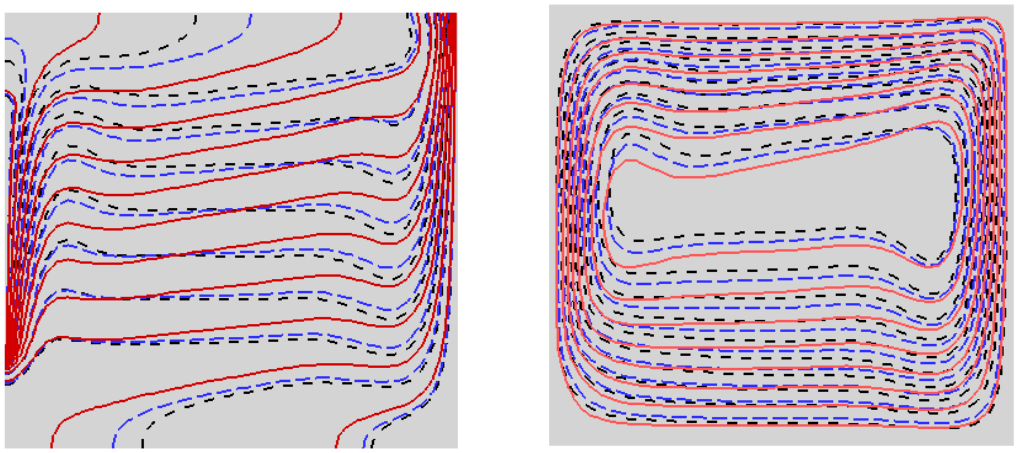

Cu-water nanofluid

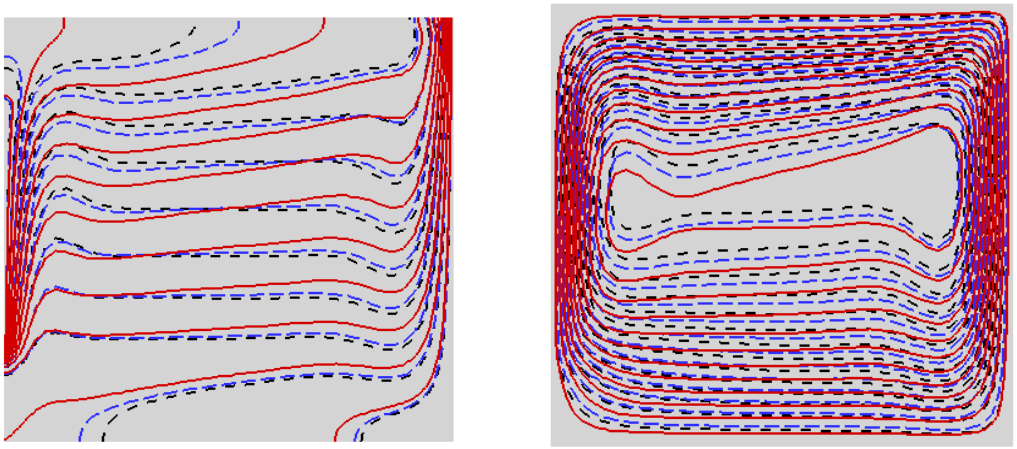

Al_2O_3-water nanofluid

Figure IV. 10. Streamlines (on the right) and isotherms (on the left) using Ha=0(- - -) Ha=30 (- - -) Ha=60 (___).

Fig. (IV.11) presents the effect of the magnetic field on temperature, vertical velocity, and radial velocity profiles along the mid-section (middle plane) of the square enclosure using different nanofluids and Ra = 10^5 , h = 0.5 and yp = 0.5. Due to buoyant flow inside the enclosure, the velocity shows a parabolic variation near the isothermal walls for Ha=0. The isotherms show a slight difference when the Hartmann value is raised to Ha=60. For both nanofluids, the radial velocity profiles is not sensitive to increasing Ha. In contrast, the vertical velocity is more significantly affected when Ha=60, its value decreasing compared to when no magnetic field is applied. This indicates that the magnetic field has a greater impact on vertical flow dynamics than on temperature distribution.

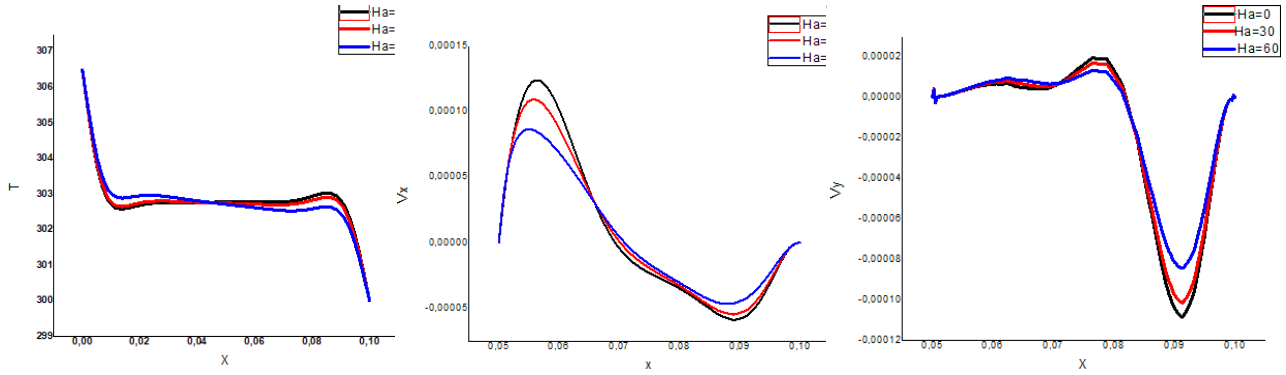

(a) Cu-water nanofluid

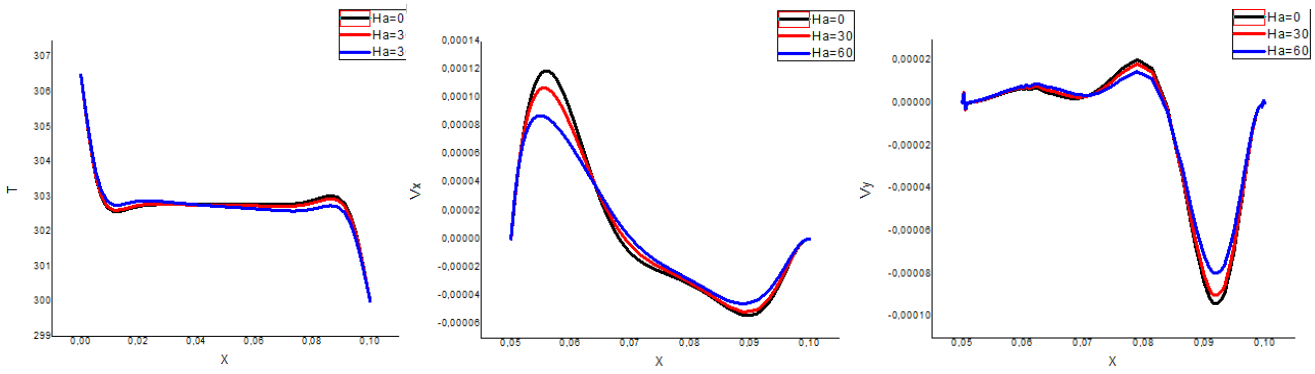

(b)Al_2O_3-water nanofluid

Figure IV. 11. Effect of Magnetic field on temperature profiles and velocity profiles (Vx, Vy) at the middle of the enclosure when Ra = 105.

For more details, Fig.(IV.12) illustrates the influence of increasing magnetic field intensity from 30 to 60. Fig. Fig.(IV.12a) shows the influence of the Hartmann number (Ha) on the local Nusselt number at the heated wall, comparing an Al_2O_3 –water nanofluid and a Copper nanofluid. The analysis indicates that the Nusselt number escalates with increasing Ha for both nanofluids. Particularly noteworthy is the more pronounced enhancement in the Al_2O_3-water nanofluid when Ha=30, while nearly identical values are observed for both nanofluids when Ha=60. An intriguing observation is that the Nusselt profile attains its peak at the same heights (y=0.02) and in (y=0.08) it reaches a minimum.

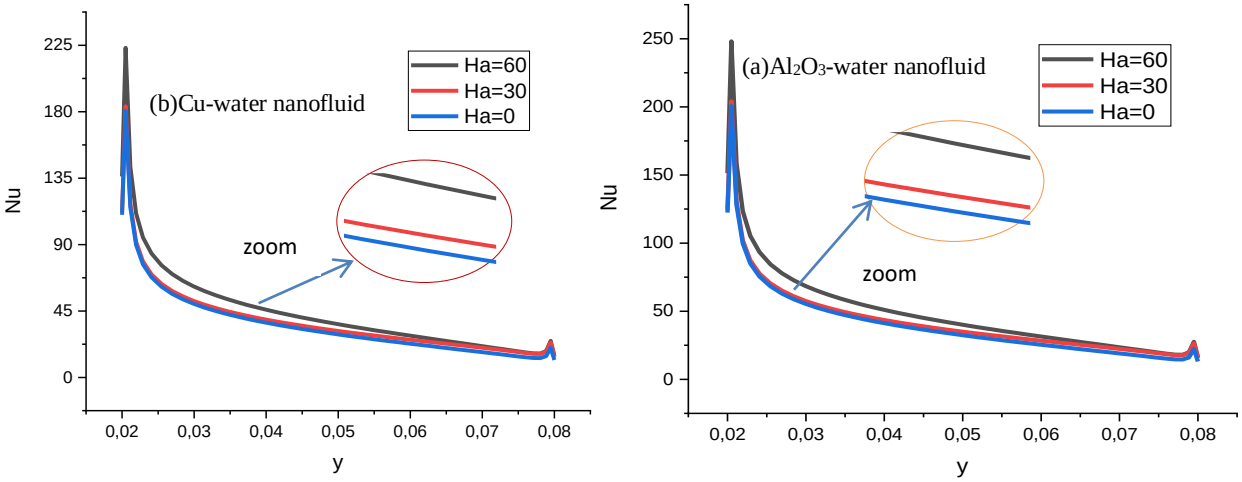

Figure IV. 12. Effect of magnetic field on local Nusselt number along the heated wall..

Conclusion

Conclusion

A numerical study has been performed to investigate the effect of using different nanofluids on the natural convection flow field and temperature distributions in a partially heated square enclosure from the left vertical wall using the finite-volume method. The analysis is given for Al_2O_3-water nanofluid, and nanofluid Copper-water nanofluid, focusing on isotherms, velocity profiles, local Nusselt, and average Nusselt numbers. The key insights from the investigation are summarized as follows:

- Both increasing the value of the Rayleigh number and Hartmann number enhances the heat transfer and flow strength keeping other parameters fixed.
- The type of nanofluid is a key factor for heat transfer enhancement. The highest values are obtained when using Cu nanoparticles.
- The introduction of a magnetic field symmetrically enhances the surface temperature distribution of nanofluid flow.
- Employing the cu water nanofluid with higher magnetic field intensities raises the azimuthal velocities in the middle of the container.
- Recommendations for future research could include exploring alterations in the orientation of the magnetic field applied to coaxial cylindrical geometries containing a rotating hybrid nanofluid flow.

References

References

[1] B. Mahfoud, Enhancement Heat Transfer of Swirling Nanofluid Using an Electrical Conducting Lid, Journal of Thermophysics and Heat Transfer 37(1) (2023) 263–271. 10.2514/1.T6550

[2] H. Shao, W. Ma, M. Kohno, Y. Takata, G. Xin, S. Fujikawa, S. Fujino, S. Bishop, X. Li, Hydrogen storage and thermal conductivity properties of mg-based materials with different structures, Int. J. Hydrog. Energy 39 (2014) 9893–9898

[3] H. Arasteh, R. Mashayekhi, D. Toghraie, A. Karimipour, M. Bahiraei, A. Rahbari, Optimal arrangements of a heat sink partially filled with multilayered porous media employing hybrid nanofluid, J. Therm. Anal. Calorim. 137 (2019) 1045–1058, https://doi.org/10.1007/s10973-019-08007-z.

[4] M.H. Esfe, H. Hajmohammad, D. Toghraie, H. Rostamian, O. Mahian, S. Wongwises, Multi-objective optimization of nanofluid flow in double tube heat exchangers for applications in energy systems, Energy 137 (2017) 160–171.

[5] L. Bouragbi, A. Salaheddine, B. Mahfoud, Analyses of entropy generation for a solar minichannel flat plate collector system using different types of nanofluids, Journal of Computational Applied Mechanics 52(4) (2021), 664-681,

[6] DOI: 10.22059/jcamech.2021.333705.662.

[7] S. Ghadikolaei, K. Hosseinzadeh, D.D. Ganji, Investigation on ethylene glycolwater mixture fluid suspend by hybrid nanoparticles (TiO2-CuO) over rotating cone with considering nanoparticles shape factor,Journal of Molecular Liquids, 272 (2018) 226–236

[8] https://doi.org/10.1016/j.molliq.2018.09.084

[9] M.H. Esfe, S. Esfandeh, M.K. Amiri, M. Afrand, A novel applicable experimental study on the thermal behavior of SWCNTs (60%)-MgO (40%)/EG hybrid nanofluid by focusing on the thermal conductivity, Powder Technology, 342, (2019) 998–1007

[10] https://doi.org/10.1016/j.powtec.2018.10.008A. Moradi D., Toghraie, A.H.M. Isfahani, A. Hosseinian, An experimental study on MWCNT–water nanofluids flow and heat

[11] transfer in double-pipe heat exchanger using porous media, Journal of Thermal Analysis and Calorimetry, 137, (2019) 1797–1807, https://doi. org/10.1007/s10973-019-08076-0.

[12] Z. Mahmood, Z. Iqbal, M. Ahmed Alyami, B. Alqahtani, M. Yassen, U. Khan, Influence of suction and heat source on MHD stagnation point flow of ternary hybrid nanofluid over convectively heated stretching/shrinking cylinder, Advances in Mechanical Engineering, 14 (2022) 1–17

[13] DOI:10.1177/16878132221126278

[14] M.Khan, M.N. Tahir, S.F. Adil, H.U. Khan, M.R. Siddiqui, M. Kuniyil, W.Tremel, Graphene based metal and metal oxide nanocomposites: Synthesis, properties and their applications, Journal of Materials Chemistry A, 3, (2015) 18753–18808.

[15] doi:10.1039/c5ta02240a.

[16] S.S. Ghadikolaeia, M. Gholiniab, 3D mixed convection MHD flow of GO- MoS2 hybrid nanoparticles in H2O– (CH2OH)2 hybrid base fluid under effect of H2 bond, International Communications in Heat and Mass Transfer, 110, (2020) 104371.

[17] Doi:10.1016/j.icheatmasstransfer.2019.104371

[18] B. Ruhani D. Toghraie M. Hekmatifar M. Hadian, Statistical investigation for developing a new model for rheological behavior of ZnO–Ag (50%–50%)/Water hybrid Newtonian nanofluid using experimental data, Physica A: Statistical Mechanics and its Applications, Vol. 525, (2019) 741–751.

[19] https://doi.org/10.1016/j.physa.2019.03.118

[20] B. Mahfoud, Magnetohydrodynamic effect on vortex breakdown zones in coaxial cylinders, European Journal of Mechanics-B/Fluids (89) (2021) 445–457

[21] https://doi.org/10.1016/j.euromechflu.2021.07.007 0997-7546

[22] H. Benhacine, B. Mahfoud, M. Salmi ,Stability effect of an axial magnetic field on fluid flow bifurcation between coaxial cylinders, International Journal of Computational Materials Science and Engineering 10(4) (2021) 2150023

[23] DOI: 10.1142/S2047684121500238

[24] B. Mahfoud., H. Benhacine, A. Laouari, A. Bendjaghlouli, Magnetohydrodynamic Effect on Flow Structures Between Coaxial Cylinders Heated from Below, Journal of Thermophysics and Heat Transfer 34(2) (2019) 1-10.

[25] https://doi.org/10.2514/1.T5805

[26] B. Mahfoud, A. Laouari, A. Hadjadj, H. Benhacine, Counter-rotating flow in coaxial cylinders under an axial magnetic field, European Journal of Mechanics-B/Fluids (78) (2019) 139-146.

[27] https://doi.org/10.1016/j.euromechflu.2019.06.009

[28] M. Azzoug, B.Mahfoud, Hibet. E. Mahfoud, Influence of External Magnetic Field on 3D Thermocapillary Convective Flow in Various Thin Annular Pools Filled with Silicon Melt, Journal of Applied Fluid Mechanics, Vol. 16 (2023) pp. 1853-1864

[29] Doi :10.47176/JAFM.16.09.1813

[30] M. Moussaoui, B. Mahfoud, Hibet E. Mahfoud, Using a Magnetic Field to Reduce Thermocapillary Convection in Thin Annular Pools, Journal of Thermophysics and Heat Transfer,37 (4) (2023)

[31] https://doi.org/10.2514/1.T6832

[32] B. Mahfoud, O.M. Azzoug, MHD effect on the thermocapillary silicon melt flow in various annular enclosures, Crystal Research & Technology, 58 (6) (2023)

[33] Doi :10.1002/crat.202300025

[34] A. Bendjaghlouli, D.E. Ameziani, B. Mahfoud, L. Bouragbi, Magnetohydrodynamic Counter Rotating Flow and Heat Transfer in a Truncated Conical Container, Journal of Thermophysics and Heat Transfer 33(3) (2019) 365-374.

[35] https://doi.org/10.2514/1.T5529

[36] H. Benhacine, B, Mahfoud, M. Salmi, Stability of conducting fluid flow between coaxial cylinders under thermal gradient and axial magnetic Field, International Journal of Thermofluid Science and Technology 9(2) (2022) 090202.

[37] https://doi.org/10.36963/IJTST.2022090202B. Mahfoud, Magnetic Field Effect on Natural ConvectioninTrapezoidal Geometry,

https://www.researchgate.net/publication/369040424, (2023).

[38] DOI: 10.13140/RG.2.2.27975.57761

[39] B. Mahfoud, Simulation of Magnetic Field Effect on Heat Transfer Enhancement of Swirling Nanofluid" International Journal of Computational Materials Science and Engineering, 11 (4) (2022) 2250007.

[40] DOI: 10.1142/S2047684122500075.

[41] B. Mahfoud, A. Bendjaghloli, Natural convection of a nanofluid in a conical container, Journal of Thermal Engineering, 4, (2018) 1713-1723.

[42] DOI:10.18186/journal-of-thermal engineering.367407

[43] B. Mahfoud, Effect of Wall Electrical Conductivity on Heat Transfer Enhancement of Swirling Nanofluid-Flow, Journal of Nanofluids, 12, (2023) 418-428.

[44] https://doi.org/10.1166/jon.2023.1932

[45] M. Mollamahdi, M. Abbaszadeh, G. A. Sheikhzadeh, Flow field and heat transfer in a channel with a permeable wall filled with Al2O3-Cu/water micropolar hybrid nanofluid, effects of chemical reaction and magnetic field, Journal of Heat and Mass Transfer Research, 3 (2016) 101- 114.

[46] M.A. Mansour, S. Sadia, R. Gorla, A.M. Rashad, Effects of heat source and sink on entropy generation and MHD natural convection of Al2O3-Cu/water hybrid nanofluid filled with square porous cavity, Thermal Science and Engineering Progress, 6, (2017) 57-71.

[47] A. Alsaedi, K. Muhammad, T. Hayat, Numerical study of MHD hybrid nanofluid flow between two coaxial cylinders, Alexandria Engineering Journal, 61 (2022) 8355–8362, https://doi.org/10.1016/j.aej.2022.01.067

[48] Y. Shagaiya Daniel., Z. Abdul Aziz, Z.Ismail, A. Bahar, F.Salah, Slip role for unsteady MHD mixed convection of nanofluid over stretching sheet with thermal radiation and electric field, Indian Journal of Physics. (2019) May:1-3.

[49] Y. Shagaiya Daniel., Z. Abdul Aziz, Z.Ismail, A. Bahar, F.Salah, Stratified electromagnetohydrodynamic flow of nanofluid supporting convective role, Korean Journal of Chemical Engineering. (2019) 1;36(7):1021-32.

[50] Y. Shagaiya Daniel., S.K. Daniel, Effects of buoyancy and thermal radiation on MHD flow over a stretching porous sheet using homotopy analysis method. Alexandria Engineering Journal.(2015) 1;54(3):705-12.

[51] Y. Shagaiya Daniel., Z. Abdul Aziz, Z.Ismail, A. Bahar, F.Salah, Entropy analysis in electrical magnetohydrodynamic (MHD) flow of nanofluid with effects of thermal radiation, viscous dissipation, and chemical reaction. Theoretical and Applied Mechanics Letters.(2017) 1;7(4):235-42.

[52] Y. Shagaiya Daniel, Z. Abdul Aziz, Z.Ismail, A. Bahar, F. Salah, Effects of slip and convective conditions on MHD flow of nanofluid over a porous nonlinear stretching/shrinking sheet. Australian Journal of Mechanical Engineering. (2018) 2;16(3):213-29.

[53] S. Manjunatha, B. AmmaniKuttan , S. Jayanthi , Ali Chamkha, B.J. Gireesha e Heat transfer enhancement in the boundary layer flow of hybrid nanofluids due to variable viscosity and natural convection. Heliyon 5 (2019) e01469.

[54] doi: 10.1016/j.heliyon.2019. e01469

[55] G. Kotha, V.R. Kolipaula, S. Rao Venkata, M. Surekha Penki and Ali J. Chamkha. Internal heat generation on bioconvection of an MHD nanofluid flow due to gyrotactic microorganisms, The European Physical Journal Plus (2020) 135(600), https://doi.org/10.1140/epjp/s13360-020-00606-2

[56] M. Veera Krishna & Ali J. Chamkha, Hall and ion slip effects on Unsteady MHD Convective Rotating flow of Nanofluids—Application in Biomedical, Engineering . Journal of the Egyptian Mathematical Society, 28 (2020)number: 1 https://doi.org/10.1186/s42787-019-0065-2

[57] F. Madani, B. Mahfoud, Hibet E. Mahfoud, Influences of electrical conductivity of the cylindrical walls on heat transfer enhancement of nanofluid swirling flow" International Journal of Thermofluid Science and Technology, 10, (2023) 100201, https://doi.org/10.36963/IJTST.2023100201

[58] H. Benhacine., B. Mahfoud.,M. Salmi, Stability of an Electrically Conducting Fluid Flow between Coaxial Cylinders under Magnetic field, Journal of Applied Fluid Mechanics, 15 (2022) 1741-1753. DOI: 10.47176/JAFM.15.02.33050